Monthly Notices
of the
ROYAL ASTRONOMICAL SOCIETY

Mon. Not. R. Astron. Soc. **416,** 101–117 (2011) doi:10.1111/j.1365-2966.2011.19014.x

Rapid optical variability of TeV blazars

Gopal-Krishna,[1⋆] Arti Goyal,[1,2] S. Joshi,[2] Chrisphin Karthick,[2] R. Sagar,[2] Paul J. Wiita,[3] G. C. Anupama[4] and D. K. Sahu[4]

[1]*National Centre for Radio Astrophysics/TIFR, Pune University Campus, Pune 411007, India*
[2]*Aryabhatta Research Institute of Observational Sciences (ARIES), Manora Peak, Nainital 263129, India*
[3]*Department of Physics, The College of New Jersey, PO Box 7718, Ewing, NJ 08628, USA*
[4]*Indian Institute of Astrophysics (IIA), Bangalore 560034, India*

Accepted 2011 May 5. Received 2011 May 3; in original form 2011 January 28

ABSTRACT

In this first systematic attempt to characterize the intranight optical variability (INOV) of TeV-detected blazars, we have monitored a well-defined set of nine TeV blazars on total 26 nights during 2004–10. In this *R*- or *V*-band-monitoring programme only one blazar was monitored per night and the minimum duration was close to 4 h, the average being 5.3 h per night. Using the CCD for strictly simultaneous photometry of the blazar and nearby reference stars (N-star photometry), an INOV detection threshold of ∼1–2 per cent was achieved in the densely sampled differential light curves derived from our data. We have further expanded the sample by including another 13 TeV blazars, taking advantage of the availability in the literature of INOV data, including those published earlier in our programme. The selection criteria for this set of 13 blazars conform to the basic criteria we had adopted for the first set of nine blazars we have monitored presently. This enlarged, well-defined representative sample of 22 TeV blazars, monitored on a total of 116 nights (including 55 nights newly reported here), has enabled us to arrive at the first estimate of the INOV duty cycle (DC) of TeV-detected blazars. Applying the conservative, but commonly employed, *C*-test, the INOV DC is found to be 59 per cent, which decreases to 47 per cent if only INOV fractional amplitudes (ψ) above 3 per cent are considered. These observations also permit, for the first time, a comparison of the INOV characteristics of the two major subclasses of TeV-detected BL Lac objects, namely low-peaked BL Lac objects (LBLs) and high-peaked BL Lac objects (HBLs), for which we find the INOV DCs to be ∼63 and 38 per cent, respectively. This demonstrates that the previously recognized INOV differential between LBLs and HBLs persists even when only their TeV-detected subsets are considered. Despite dense sampling, the intranight light curves of the 22 TeV blazars have not revealed even a single feature on time-scale substantially shorter than 1 h, even though the inner jets of TeV blazars are believed to have exceptionally large bulk Lorentz factors (and correspondingly stronger time compression). An intriguing feature, clearly detected in the light curve of the HBL J1555+1111, is a 4 per cent 'dip' on a 1 h time-scale. This unique feature could have arisen from absorption in a dusty gas cloud, occulting a superluminally moving optical knot in the parsec-scale jet of this relatively luminous BL Lac object.

Key words: galaxies: active – BL Lacertae objects: general – galaxies: jets – galaxies: photometry.

1 INTRODUCTION

Intensity variations have long been recognized as a defining characteristic of active galactic nuclei (AGNs). Variability is a powerful tool for probing AGN geometry and physical properties such as the black hole mass, and the sizes and bulk motions of the outflows in their innermost regions that are well beyond the current imaging capabilities of telescopes in any part of the electromagnetic spectrum (e.g. Urry & Padovani 1995; Wagner & Witzel 1995; Xie et al. 2001). The variations can be particularly violent for those AGNs whose flux is dominated by relativistic jets of non-thermal radiation broadly pointing in our direction (e.g. Begelman,

⋆E-mail: krishna@ncra.tifr.res.in

Blandford & Rees 1984). Intensities of such AGNs, called 'blazars', are known to vary across the entire electromagnetic spectrum and time-scales from minutes to years have been observed. For instance, in the soft X-ray band, several TeV-emitting blazars have been found to vary on a characteristic time-scale of $\sim$1 d, with the flares having substructures on shorter time-scales of $\sim 10^4$ s (e.g. Kataoka et al. 2001; Tanihata et al. 2001). In the optical regime, there have been many detections of intranight optical variability (INOV), or optical microvariability, following the pioneering work of Carini, Miller & Goodrich (1990), who first used CCD detectors as multi-object photometers for this purpose. The shortest time-scale found for essentially all INOV events is around 1 h, with an amplitude of a few per cent (e.g. Xie et al. 2001; Romero et al. 2002; Stalin et al. 2004a). Such rapid continuum variability of blazars is usually explained by invoking relativistic jets (e.g. Marscher 1996; Schlickeiser 1996; Wiita 2006).

A study of 23 AGNs of the quasar/Seyfert1 type (i.e. non-blazar) yielded a 1σ upper limit of 0.03 mag for variability on hour-like time-scales (Webb & Malkan 2000). The literature does contain reports of a few INOV detections on time-scales much shorter than 1 h. Examples include the papers by Kidger & deDiego (1990), Sagar, Gopal-Krishna & Wiita (1996), Xie et al. (2001) and Dai et al. (2001); however, see Romero et al. (2002) for a convincing critique of the latter two claims. To our knowledge, such assertions are lacking in the literature over the past five years or so, aside from a very recent paper presenting evidence for a quasi-periodic oscillation of $\simeq$15 min spanning most of a night of optical monitoring of the TeV blazar S5 0716+714 (Rani et al. 2010), which is also a member of our present sample. Very recently, Impiombato et al. (2011) have reported a single event of duration $\sim$25 min in J band while searching for long- and short-term optical and infrared variabilities for blazar PKS0537−441 in the data spanning for $\sim$6 yr (2004–09). There is thus a need for renewed efforts capable of making robust detections of events of ultrarapid INOV events on subhour time-scales.

Since γ-ray emission is known to be correlated with relatively large bulk Doppler factors of the radiating plasma in the blazar jets for both the GeV band probed by Energetic Gamma Ray Experiment Telescope (EGRET; e.g. Kellermann et al. 2004; Lister & Homan 2005) and the higher energies probed by *Fermi*/Large Area Telescope (*Fermi*/LAT; Kovalev et al. 2009; Savolainen et al. 2010), TeV blazars appear to be particularly promising candidates for detecting the most rapid INOV. In TeV blazars, the relativistic plasma of the inner jets almost certainly must move with a bulk Lorentz factor $\Gamma \geq 45$–50 in order to escape absorption of the TeV photons due to the pair production process in the radiation field present near the origin (e.g. Krawczynski, Coppi & Aharonian 2002; Begelman, Fabian & Rees 2008; for large Lorentz factors in blazar jets, also see Kundt & Gopal-Krishna 1980, 2004). According to one model, such ultrafast moving emission features may arise *in situ* within the jet, e.g. from reconnection events in a Poynting flux dominated jet (Giannios, Uzdensky & Begelman 2009). Thus, it seems likely that in TeV blazars the bulk Lorentz factors of the optically radiating inner segments of the jets are also comparatively larger than those occurring in other blazars. Here we note that the marked paucity of apparent superluminal motion in the jets of TeV blazars, highlighted by Piner & Edwards (2004), can be reconciled with the above requirement of extreme bulk Lorentz factors in a number of ways, e.g. by taking into account a modest opening angle for the jet (Gopal-Krishna, Dhurde & Wiita 2004; Gopal-Krishna, Wiita & Dhurde 2006; Gopal-Krishna et al. 2007; Petrucci, Boutelier & Henri 2011), or by postulating a spine-sheath geometry for the subparsec-scale jets (e.g. Attridge, Roberts & Wardle 1999; Ghisellini, Haardt & Matt 2004) or, alternatively, if the bulk of the γ-rays come from an ultrarelativistically approaching volume element in the jet (e.g. Giannios et al. 2009; also, Gopal-Krishna, Singal & Krishnamohan 1984).

In Section 2, we describe the selection of our sample of TeV blazars for intranight optical monitoring. Our observations are described in Section 3 and the results summarized in Section 4, followed by a discussion in Section 5.

2 SAMPLE SELECTION FOR TeV BLAZARS

Our sample of TeV blazars consists of two sets. Set 1 is derived from the list of TeV-detected extragalactic AGNs, published by Weekes (2008, table 2 of his paper). Application of the criteria, $z > 0.1$, $\delta > -10^\circ$ and $m_B \leq 18$ to that list leave us with nine TeV blazars. The redshift limit is designed to exclude the nearest blazars so that the optical image should have a point-like appearance. This is to ensure that the host galaxy makes a negligible contribution to the image, a pre-requisite for high-precision photometry. The declination and the apparent magnitude limits are meant to ensure a sufficiently dense sampling and reasonably long duration ($\gtrsim$4 h) for the continuum light curves obtained with the 1–2 m class telescopes employed in this programme. The nine TeV blazars constituting set 1 are TeV1219+283, TeV1429+427, TeV0809+524, TeV1218+304, TeV1011+496, TeV0716+714, TeV1553+11, TeV0219+425 and TeV1256−058, listed in increasing order of distance from us. The intranight and long-term optical light curves of these nine blazars are derived in this study and presented here.

Our set 2 of TeV blazars was derived from table 1 of Abdo et al. (2010a), consisting of 709 TeV-detected AGNs, which is based on 11 months of monitoring with *Fermi* LAT. This set consists of 13 blazars, including 10 high-polarization core-dominated quasars (HPCDQs) and three BL Lac objects. The HPCDQs were selected employing the following criteria: all CDQs labeled 'HP' ($P_{\rm op} > 3$ per cent) in the compendium of Véron-Cetty & Véron (2006) were subjected to the aforementioned selection criteria, namely $z > 0.1$, $\delta > -10^\circ$ and $m_B \leq 18$. To ensure the availability of INOV data additional selection filters used are as follows.

(a) We selected all the seven HPCDQs from Noble (1995, table 3.1). These are J0239+1637, J1159+2914, J1256−0547, J1310+3220, J1643+3953, J2225−0457 and J2253+1608. Of these J1256−0547 (3C 279) is already a member of set 1 and J1643+3953 (3C 345) is undetected by *Fermi* LAT. This gave us the first five TeV blazars for set 2.

(b) Another three HPCDQs were taken from the polarimetric survey of Wills et al. (1992), limiting ourselves to the right ascension range $3^{\rm h}$–$15^{\rm h}$ and declination range -10° to $+40^\circ$. Note that although these criteria yielded five HPCDQs (J0423−0120, J0739+0136, J1058+0133, J1159+2914 and J1256−0547), the last two of these are already a part of the Noble (1995) sample (a). This left us with three additional blazars.

(c) One HPCDQ, J1218−0119, was taken from the first phase of our INOV programme (Sagar et al. 2004; Stalin et al. 2005). INOV data have been taken from those papers for this source as well as for another two HPCDQs (J0239+1637 and J1310+3220) that are in the part (a) of set 2 derived from Noble (1995). Note that there were only three HPCDQs monitored in the first phase of our INOV programme.

(d) Lastly, one HPCDQ was added from the sample of Romero, Cellone & Combi (1999). They have reported V-band intranight

Table 1. The sample of 22 TeV blazars studied in the present work.

IAU name	Other name	Type	RA (J2000) (h m s)	Dec. (J2000) (° ′ ″)	B	M_B	z	$P_{\rm op}$ (per cent)	$\alpha_{\rm r}$	$P_{\rm c}^{5\,\rm GHz}$ (W Hz^{-1})	$P_{\rm ext}^{5\,\rm GHz}$ (W Hz^{-1})	log $f_{\rm c}$	log R^*	$\beta_{\rm app}$ (max)
(1)	(2)	(3)	(4)	(5)	(6)	(7)	(8)	(9)	(10)	(11)	(12)	(13)	(14)	(15)
Set 1														
J0222+4302	3C 66A	IBL	02 22 39.6	+43 02 08	15.71	−24.96	0.444	16.8[a]	−0.20[§]	6.5×10^{26}[h]	1.1×10^{27}	−0.22	2.98	5.8[n]
J0721+7120	S5 0716+71	IBL	07 21 53.3	+71 20 36	15.50	−24.73	0.310	29.0[b]	+0.36	1.0×10^{27}[i]	4.5×10^{26}	0.36	2.43	10.07[o]
J0809+5218	1ES 0806+524	HBL	08 09 49.2	+52 18 58	15.30	−23.25	0.138		−0.25	5.6×10^{24}[j]	2.7×10^{24}	0.30	1.79	
J1015+4926	GB 1011+496	HBL	10 15 04.2	+49 26 01	16.56	−22.88	0.200		−0.26	2.0×10^{25}[k]	1.8×10^{25}	0.03	2.59	
J1221+3010	PG 1218+304	HBL	12 21 21.9	+30 10 37	16.50	−22.72	0.182	6.6[e]	−0.08	5.4×10^{24}[j]	1.3×10^{24}	0.58	1.85	
J1221+2813	ON 231	HBL	12 21 31.7	+28 13 58	16.81	−21.21	0.102	4.3[e]	−0.09[§]	1.5×10^{25}[i]	3.1×10^{24}	0.70	3.01	3.2[q]
J1256−0547	3C 279	FSRQ	12 56 11.1	−05 47 21	18.01	−23.24	0.538	44.0[b]	+0.48[§]	3.2×10^{28}[i]	1.0×10^{28}	0.50	4.51	20.58[o]
J1428+4240	H 1426+428	HBL	14 28 32.7	+42 40 21	16.95	−21.60	0.129	2.5[d]	−0.58	1.5×10^{24}[j]	7.2×10^{23}	0.34	1.96	2.09[r]
J1555+1111	PG 1553+11	HBL	15 55 43.1	+11 11 24	15.00	−25.42	0.360‡	3.5[g]	+0.54	1.5×10^{26}[m]	1.9×10^{25}	0.88	1.85	
Set 2														
J0238+1637	AO 0235+164	LBL	02 38 38.9	+16 37 00	16.46	−25.47	0.940	43.9[b]	+0.71[§]	1.3×10^{28}[i]	2.1×10^{27}	0.80	3.12	
J0423−0120	PKS 0420−01	FSRQ	04 23 15.8	−01 20 33	17.50	−24.17	0.915	20.0[b]	+0.19[§]	8.2×10^{28}[i]	4.4×10^{28}	0.27	3.69	7.35[o]
J0738+1742	PKS 0735+17	LBL	07 38 07.4	+17 42 19	16.76	−24.04	>0.424	36.0[b]	−0.28[§]	1.5×10^{27}[i]	3.6×10^{26}	0.61	3.40	11.8[p]
J0739+0137	PKS 0736+01	FSRQ	07 39 18.0	+01 37 04	16.90	−21.96	0.191	5.6[c]	−0.10[§]	2.2×10^{26}[i]	1.3×10^{25}	1.20	3.45	14.44[o]
J0854+2006	OJ 287	LBL	08 54 48.8	+20 06 30	15.91	−24.30	0.306	37.2[b]	+0.20[§]	1.6×10^{27}[i]	6.2×10^{26}	0.41	2.91	11.70[o]
J1058+0133	PKS 1055+01	FSRQ	10 58 29.6	+01 33 58	18.74	−23.34	0.888	5.0[d]	+0.06[§]	3.9×10^{28}[i]	1.1×10^{28}	0.54	4.26	11.0[o]
J1159+2914	4C 29.45	FSRQ	11 59 31.9	+29 14 45	14.80	−27.00	0.729	28.0[b]	−0.34[§]	1.3×10^{28}[i]	3.6×10^{27}	0.57	2.60	24.8[o]
J1217+3007	B2 1215+30	HBL	12 17 52.0	+30 07 01	16.07	−22.45	0.130	8.0[e]	−0.12[§]	1.3×10^{25}[j]	8.8×10^{24}	0.17	2.60	
J1218−0119	PKS 1216−010	BL[£]	12 18 34.9	−01 19 54.0	16.17	−25.14	0.554	6.9[f]	+0.01[§]	4.3×10^{27}[l]	2.5×10^{27}	0.22	3.01	
J1310+3220	B2 1308+32	FSRQ	13 10 28.7	+32 20 44	15.61	−26.69	0.997	28.0[b]	−0.09[§]	3.0×10^{28}[i]	9.9×10^{27}	0.49	2.71	27.2[o]
J1512−0906	PKS 1510−08	FSRQ	15 12 50.5	−09 06 00	16.74	−23.49	0.360	7.8[b]	−0.10[§]	1.7×10^{27}[i]	7.7×10^{25}	1.35	3.48	20.2[o]
J2225−0457	3C 446	FSRQ	22 25 47.2	−04 57 01	18.83	−23.66	1.404	17.3[b]	−0.13[§]	1.3×10^{29}[i]	6.2×10^{28}	0.34	4.58	17.34[o]
J2253+1608	3C 454.3	FSRQ	22 53 57.7	+16 08 53	16.57	−25.11	0.859	16.0[b]	−0.28[§]	6.7×10^{28}[i]	1.2×10^{28}	0.74	3.99	14.19[o]

Columns are as follows: (1) source name; (2) most popular name as given in Véron & Véron (2006); (3) classification into low-, intermediate- or high-frequency peaked blazars or flat spectrum radio quasar (FSRQ); (4) right ascension; (5) declination; (6) apparent B magnitude; (7) absolute B magnitude; (8) redshift; (9) the measured optical polarization; (10) radio spectral index; (11) radio core luminosity; (12) extended emission radio luminosity; (13) radio core dominance parameter f_c (see text); (14) radio loudness R^* is the K-corrected rest-frame ratio of the 5 GHz to 2500 Å flux densities, following Stocke et al. (1992) [reference for the radio flux is Véron-Cetty & Véron (2006)]; (15) the fastest apparent speed observed in the parsec-scale jet (in units of the speed of light).

[£]Abdo et al. (2010a); SED classification is not available.

‡Reference for redshift: Rector et al. (2003), see also, Treves, Falomo & Uslenghi (2007).

[a]Takalo, Sillanpää & Nilsson (1994); [b]Fan et al. (1997); [c]Stockman, Moore & Angel (1984); [d]Jannuzi, Smith & Elston (1993); [e]Wills et al. (1992); [f]Visvanathan & Wills (1998); [g]Andruchow, Romero & Cellone (2005).

[§]The radio spectral index derived using simultaneous flux measurements from Kovalev et al. (1999) by means of the least-squares method ($S_\nu \propto \nu^\alpha$). The remaining values of $\alpha_{\rm r}$ have been calculated using 6 and 20 cm. flux densities from Véron-Cetty & Véron (2006).

Reference for VLBI flux: [h]Marscher et al. (2002); [i]Kovalev et al. (2005); [j]Giroletti et al. (2006); [k]Helmboldt et al. (2007); [l]Wehrle, Morabito & Preston (1984); [m]Rector et al. (2003).

Reference for $\beta_{\rm app}$: [n]Britzen et al. (2008); [o]Lister et al. (2009b); [p]Britzen et al. (2010); [q]Kellermann et al. (2004); [r]Piner, Pant & Edwards (2008).

monitoring of a sample of the southern AGN that contains four HPCDQs according to the Véron-Cetty & Véron (2006) classification. These are J0538−4405, J1147−3812, J1246−2547 and J1512−0906. Only the last of these HPCDQs was included in our sample because we could ensure a minimum three nights' monitoring data; the others are situated far to the south.

(e) We have also included three BL Lac objects PKS 0735+178, OJ 287 and B2 1215+30 for which intranight monitoring data of duration $\gtrsim$4 h are available in the literature. This completes our set 2 that contains 13 TeV-detected blazars.

Salient properties of the two blazar sets are listed in Table 1. All these sources have flat radio spectra [$\alpha_{\rm r} > -0.5$, where $S(\nu) \propto \nu^{\alpha_{\rm r}}$] as well as high-optical linear polarization, with $P_{\rm op}$ falling in the range 3.5–44 per cent, except for J1428+4240 (which has a slightly steep integrated radio spectrum with $\alpha_{\rm r} \simeq -0.58$, and a comparatively low-optical polarization, $P_{\rm op} = 2.5$ per cent). The values of radio core luminosity ($P_{\rm c}$), extended radio luminosity ($P_{\rm ext}$) and the radio core dominance parameter ($f_{\rm c}$; ratio of core to extended radio luminosities) at 5 GHz were determined using the available Very Long Baseline Interferometry (VLBI) measurements at milliarcsecond resolution and the integrated National Radio Astronomy Observatory (NRAO) VLA Sky Survey (NVSS) flux values at 1.4 GHz, taking a radio spectral index of zero for the core ($\alpha_c = 0$) and $\alpha_{\rm ext} = -0.5$ for the extended emission. The concordance cosmological model was assumed with a Hubble constant $H_0 = 70$ km s^{-1} Mpc^{-1}, $\Omega_m = 0.3$ and $\Omega_\Lambda = 0.7$ (Spergel et al. 2007). Values of the radio loudness parameter (R^*) were determined following Stocke et al. (1992). The absolute magnitudes, M_B, were calculated taking the total galactic extinction from Schlegel, Finkbeiner & Davis (1998) and assuming an optical spectral index $\alpha_{\rm op}$ of −0.7.

3 OBSERVATIONS

3.1 Instruments used

The observations were mainly carried out using the 104-cm Sampurnanand telescope (ST) located at the Aryabhatta Research Institute of Observational Sciences (ARIES) in Nainital, India. It has Ritchey–Chrétien (RC) optics with an f/13 beam (Sagar 1999). The detector was a cryogenically cooled 2048 × 2048 chip mounted at

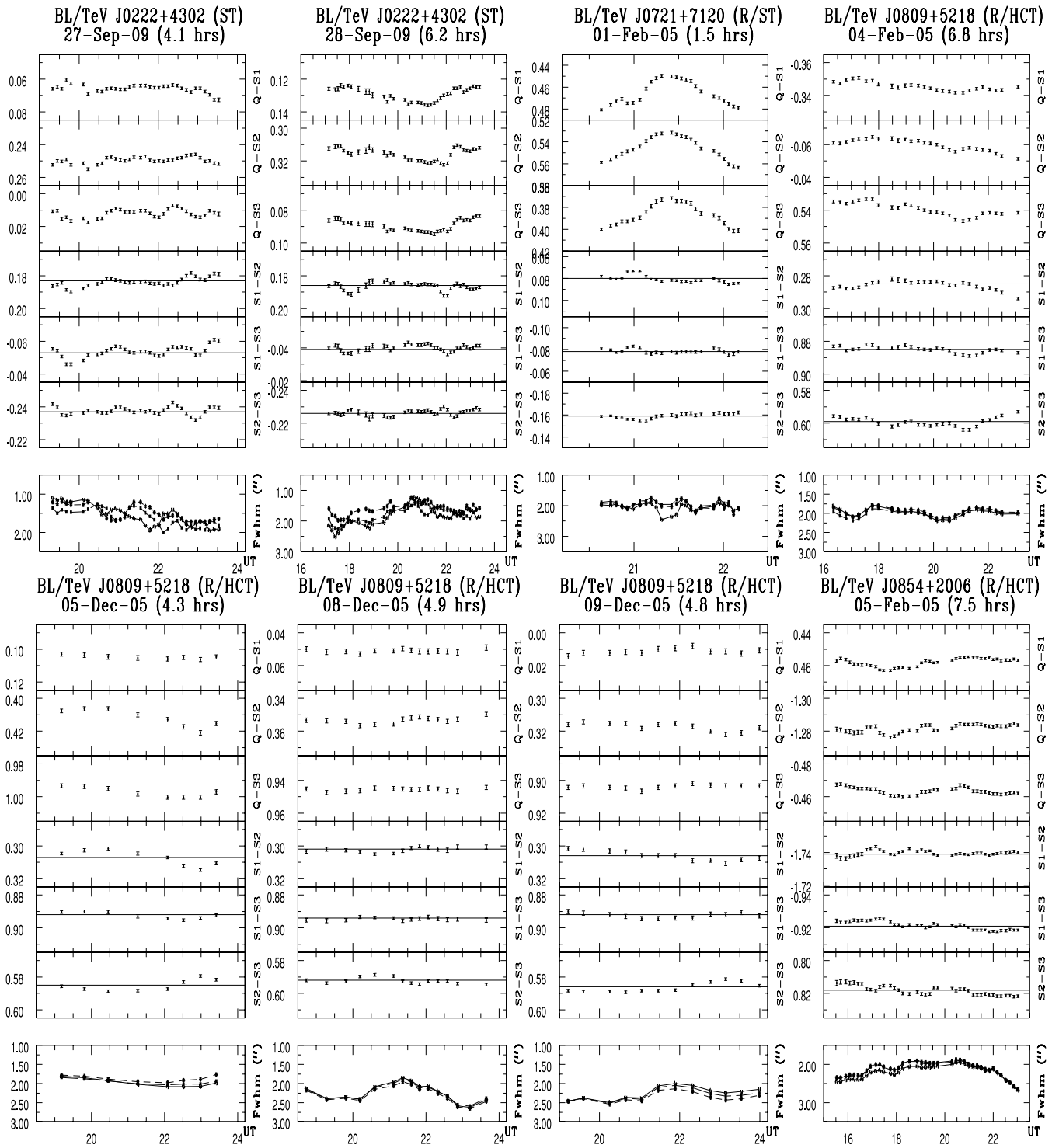

Figure 1. Intranight DLCs of the nine TeV blazars (set 1) and J0854+2006 (set 2) monitored in the present study. The source name, date of monitoring, its duration, the filter and the telescope used are mentioned at the top of each frame. For each night the bottom panel shows the variation of the atmospheric seeing through the monitoring duration.

the Cassegrain focus. This chip has a readout noise of 5.3 e^- $pixel^{-1}$ and a gain of 10 e^- per analog to digital unit (ADU) in the usually employed slow readout mode. Each pixel has a dimension of 24 μm^2 which corresponds to 0.37 $arcsec^2$ on the sky, covering a total field of 13×13 $arcmin^2$. Observations were carried out in 2×2 binned mode to improve the signal-to-noise ratio. All the observations with the ST were carried out using an *R* filter for which the CCD sensitivity is maximum. The seeing ranged mostly between ∼1.5 and 3 arcsec, as determined using three moderately bright stars within the CCD frame. For each night, the plot of seeing is provided in Fig. 1 in the corresponding bottom panel.

The other telescope used for our monitoring of TeV blazars is the 201-cm Himalayan Chandra Telescope (HCT) of the Indian Astronomical Observatory (IAO) located at Hanle, India, which is

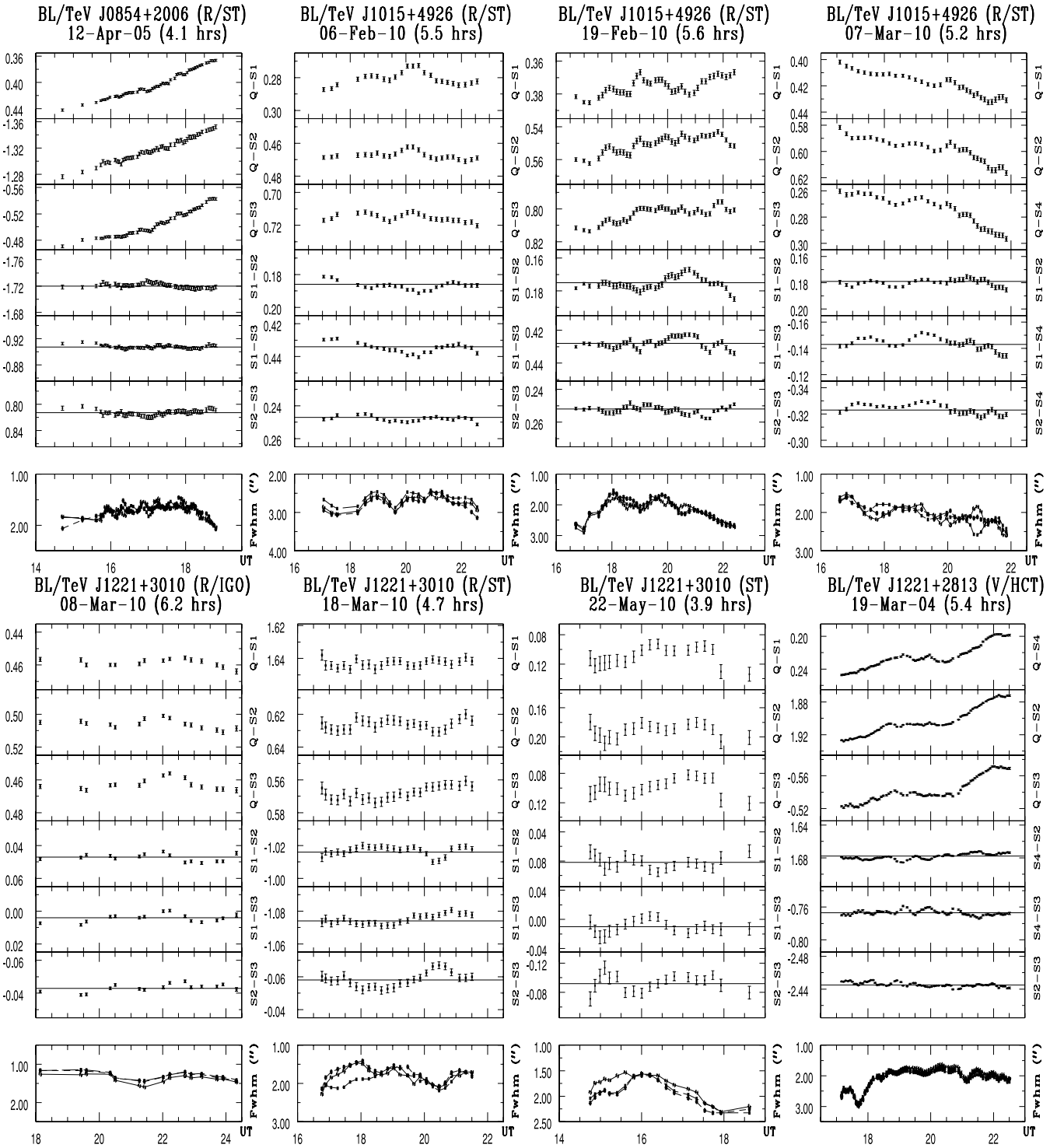

Figure 1 – *continued*

also of the RC design with an $f/9$ beam at the Cassegrain focus.[1] The detector was a cryogenically cooled 2048 × 4096 chip, of which the central 2048 × 2048 pixels were used. As the pixel size is 15 μm^2 the image scale of 0.29 arcsec pixel^{-1} covers an area of 10 × 10 arcmin^2 on the sky. The readout noise of the CCD is 4.87 e$^-$ pixel^{-1} and the gain is 1.22 e$^-$ ADU^{-1}. This CCD was used in an unbinned mode. The seeing ranged mostly between ∼1 and 3 arcsec.

Lastly, blazar monitoring data of one night were obtained using the 200-cm The Inter-University Centre for Astronomy and Astrophysics (IUCAA) Girawali Observatory (IGO) telescope located near Pune, India. It has an RC design with an $f/10$ beam

[1] http://www.iiap.res.in/∼iao

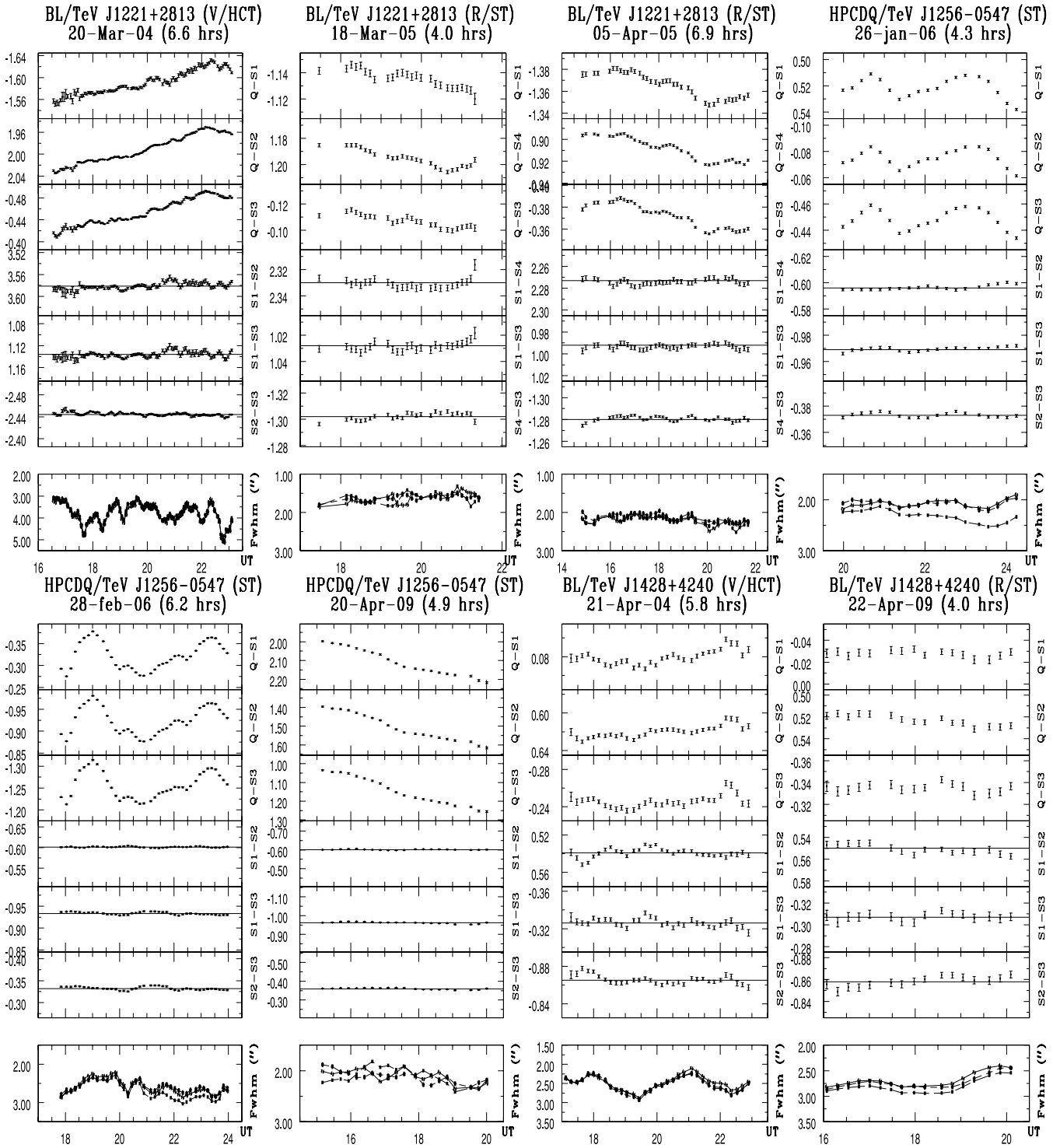

Figure 1 – *continued*

at the Cassegrain focus.[2] The detector was a cryogenically cooled 2110 × 2048 chip mounted at the Cassegrain focus. The pixel size is 15 μm^2 so that the image scale of 0.27 arcsec $pixel^{-1}$ covers an area of 10 × 10 $arcmin^2$ on the sky. The readout noise of this CCD is 4.0 e^- $pixel^{-1}$ and the gain is 1.5 e^- ADU^{-1}. The CCD was used in an unbinned mode. The seeing ranged between ∼1.0 and ∼1.5 arcsec on that particular night.

The observations were made using *R* or *V* filters. The exposure times were typically 10–12 min for the ARIES and IGO observations and ranged between 3 and 6 min for the observations from the IAO (depending on the brightness of the source, the lunar phase and the sky transparency for the night). The field positioning was adjusted so as to always have within the CCD frame two to three

[2] http://www.iucaa.ernet.in/\%7Eitp/igoweb/igo_tele_and_inst.htm

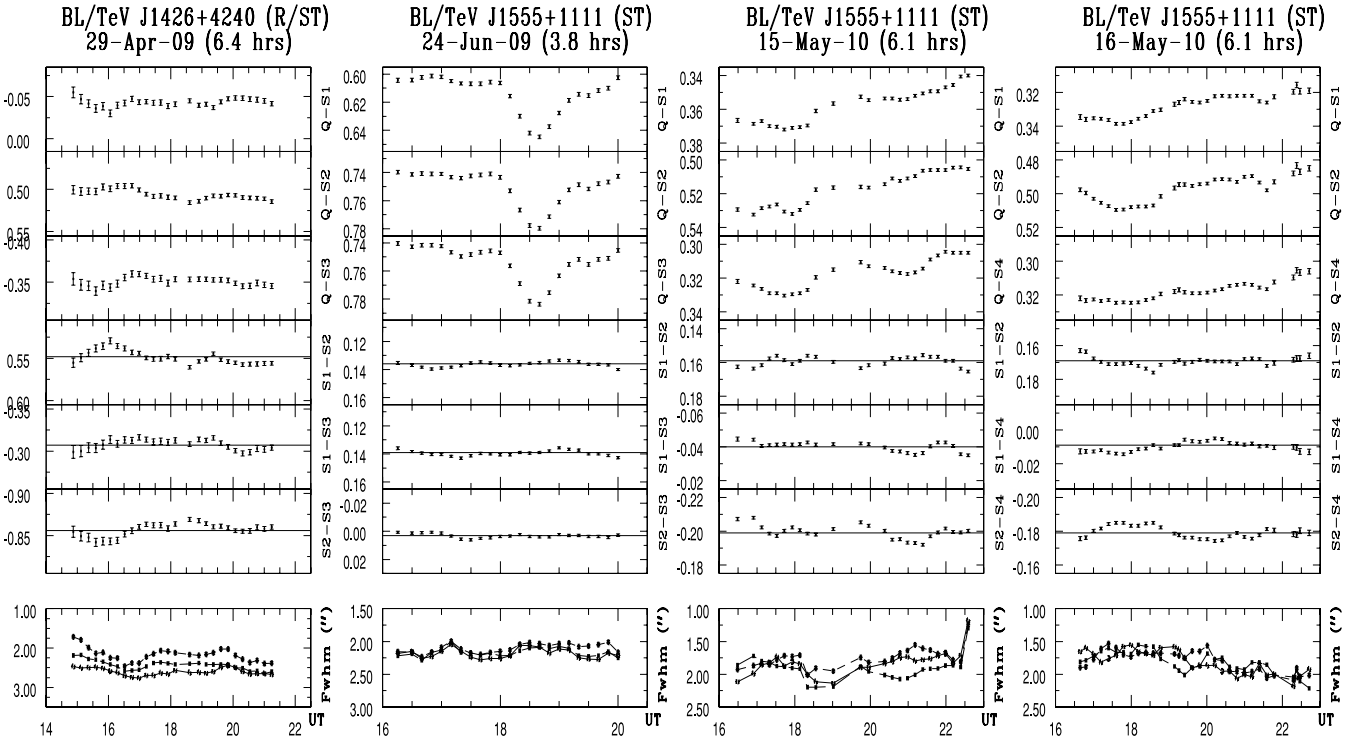

Figure 1 – *continued*

comparison stars within about a magnitude of the blazar in order to minimize the possibility of getting spurious variability detection (e.g. Cellone, Romero & Araudo 2007). For all three telescopes, bias frames were taken intermittently and twilight sky flats were obtained on each night. Each blazar in set 1 was monitored for a minimum of three nights. Likewise, for the blazars in set 2, this requirement of minimum three nights is met, except for the case of J2253+1608 (3C 454.3) for which only two nights' monitoring data are available.

3.2 Data reduction

The pre-processing of the images (bias subtraction, flat-fielding and cosmic ray removal) was done by applying the standard procedures in IRAF[3] and MIDAS[4] software programs. The instrumental magnitudes of the blazar and the comparison stars in the image frames were determined by aperture photometry using DAOPHOT II[5] (Stetson 1987). The magnitude of the blazar was measured relative to the steady comparison stars present on the same CCD frame (Table 2). In this manner, differential light curves (DLCs) of each blazar were produced relative to three comparison stars (Fig. 1). For each night, the selection of optimum aperture size for the photometry was done by examining the observed dispersions in the star–star DLCs for different aperture radii starting from the median seeing (full width at half-maximum) value on that night to four times that value. We selected the aperture that showed minimum scatter for the steadiest DLC found for the various pairs of the comparison stars (e.g. Stalin et al. 2004a).

[3] Image Reduction and Analysis Facility (http://iraf.noao.edu/).
[4] Munich Image and Data Analysis System (http://www.eso.org/sci/data-processing/software/esomidas/).
[5] Dominion Astrophysical Observatory Photometry software.

4 RESULTS

4.1 Variability criteria and duty cycles

The INOV DLCs are shown in Fig. 1 for all the nine blazars of set 1. From set 2 we present here the DLCs for just J0854+2006 (OJ 287) since it is also monitored in the present work (Fig. 1). The DLCs for another few members of set 2, which too were monitored in the present work, can be found in Goyal et al. (2011) as they form part of the samples discussed in that paper. Fig. 2 displays the long-term optical variability (LTOV) DLCs for sources that could be observed in the same colour filter on a minimum of three nights. Table 3 summarizes the observations and derived results for our entire sample of 22 TeV blazars, nine of which were monitored in the present study (set 1), while for the remainder (set 2) the INOV data were largely taken from the literature (Section 2; Table 3). The sixth, seventh and eighth columns give, respectively, the monitoring duration on the respective night, the number of data points ($N_{\rm points}$) in the DLC and the rms of the steadiest star–star DLC obtained using two of the comparison stars.

The next columns in Table 3 contain the measures of the source variability (INOV) on each night. The fractional amplitude of INOV, ψ, is given in Column 9, while $C_{\rm eff}$, a widely used indicator of variability status, is given in Column 10. The classification 'variable' (V) or 'non-variable' (N) as decided using the C-test, basically defined following the criteria of Jang & Miller (1997), is given in Column 11.

$C_{\rm eff}$ for a night is derived by combining the C-values estimated for individual DLCs of the blazar on that night. For a given DLC, C is defined as the ratio of its standard deviation, σ_T and $\eta\sigma_{\rm err}$, where $\sigma_{\rm err}$ is the average of the rms errors of its individual data points. As the photometric errors given by the DAOPHOT/IRAF package is known to be underestimated, a compensatory factor η is determined that would make the rms of the DLC consistent with the rms of its

Table 2. Positions and apparent magnitudes[a] of the TeV blazars and the comparison stars.

Source	Set no.	RA (J2000) ($^{h\,m\,s}$)	Dec. (J2000) ($^{\circ}\,'\,''$)	B^a (mag)	R^a (mag)	$B-R$ (mag)
J0222+4302	1	02 22 39.61	+43 02 07.9	14.94	14.35	0.59
S1		02 22 28.41	+43 03 40.9	14.59	14.00	0.59
S2		02 22 20.45	+42 57 18.7	14.74	13.66	1.08
S3		02 22 39.09	+42 57 05.5	14.69	13.94	0.75
J0238+1637	2	02 38 38.92	+16 36 59.2	18.65	15.92	2.73
S1		02 38 56.00	+16 37 43.0	17.43	16.60	0.83
S2		02 38 38.52	+16 40 05.3	18.37	16.61	1.76
S3		02 38 22.25	+16 39 41.8	17.37	16.22	1.15
J0721+7120	1	07 21 53.39	+71 20 36.7	15.15	14.27	0.88
S1		07 22 12.58	+71 21 15.2	14.49	13.78	0.71
S2		07 21 54.31	+71 19 21.2	14.46	13.67	0.79
S3		07 21 13.95	+71 17 10.0	14.45	13.55	0.90
J0809+5218	1	08 09 49.20	+52 18 58.4			
S1		08 09 43.90	+52 18 09.5	16.17	15.47	0.70
S2		08 10 16.45	+52 19 16.9	17.85	16.10	1.75
S3		08 09 52.68	+52 16 15.1	15.25	14.73	0.52
J1015+4926	1	10 15 04.13	+49 26 00.8	15.32	14.58	0.74
S1		10 15 29.71	+49 30 41.5	15.27	14.84	0.43
S2		10 15 37.87	+49 28 19.2	14.92	14.56	0.36
S3		10 15 08.03	+49 25 42.3	14.27	13.55	0.72
S4		10 15 39.84	+49 29 25.7	16.70	14.95	1.75
J1221+3010	1	12 21 21.93	+30 10 37.2	16.13	14.93	1.20
S1		12 21 22.62	+30 09 53.8	16.72	15.43	1.29
S2		12 21 23.08	+30 10 38.9	17.04	15.42	1.62
S3		12 21 37.05	+30 10 18.3	16.28	15.52	0.76
J1221+2813	1	12 21 31.69	+28 13 58.4	14.65	14.24	0.41
S1		12 21 26.01	+28 12 30.9	16.94	15.91	1.03
S2		12 21 13.86	+28 13 04.5	13.61	12.88	0.73
S3		12 21 11.81	+28 11 53.7	16.13	15.00	1.13
J1256−0547	1	12 56 11.19	−05 47 21.5	17.39	15.87	1.52
S1		12 56 26.61	−05 45 22.8	15.22	14.75	0.47
S2		12 55 58.00	−05 44 18.9	16.19	15.30	0.89
S3		12 56 14.48	−05 46 47.8	16.39	15.43	0.96
J1428+4240	1	14 28 32.62	+42 40 21.4			
S1		14 28 08.06	+42 40 37.4	16.62	16.23	0.39
S2		14 28 07.38	+42 44 20.0	16.16	15.74	0.42
S3		14 28 16.05	+42 40 39.9	16.77	16.56	0.21
J1555+1111	1	15 55 43.05	+11 11 24.3	14.30	13.99	0.31
S1		15 55 46.08	+11 11 19.6	14.52	13.62	0.90
S2		15 55 52.17	+11 13 18.5	14.47	13.56	0.91
S3		15 55 40.77	+11 04 44.7	14.46	13.56	0.90
S4		15 56 06.02	+11 13 44.9	15.44	14.54	0.90
J0854+2006	2	08 54 48.68	+20 06 30.8	15.95	15.56	0.40
S1		08 54 53.36	+20 04 45.1	15.25	13.97	1.28
S2		08 54 41.29	+20 06 43.2	16.86	15.60	1.26
S3		08 54 55.19	+20 05 42.4	15.83	14.94	0.89

[a]Monet et al. (2003)

individual data points (see Edelson et al. 2002; also, Stalin et al. 2004a). In this way, the computed value of η is found to be $\sim$1.5 (Gopal-Krishna et al. 2003; Sagar et al. 2004; Stalin et al. 2004a,b, 2005). However, our analysis for the present data set yields $\eta = 1.3$ and so we have adopted this value here. We computed $C_{\rm eff}$ from the C values (as defined above) derived for the individual DLCs of a given blazar relative to three different comparison stars which were monitored simultaneously with the blazar on the same CCD chip. This gave us three values of C for a given blazar. These values were converted into probabilities and multiplied to obtain $C_{\rm eff}$ for the blazar (see Sagar et al. 2004 for details). This has the advantage of using the available multiple DLCs of an AGN, relative to different comparison stars. The AGN is termed 'V' for $C_{\rm eff} > 2.576$, corresponding to a nominal confidence level above 0.99. The 'probable variable' (PV) classification applies when $1.950 < C_{\rm eff} < 2.576$, corresponding to a nominal confidence level between 0.95 and 0.99.

It has been recently argued by de Diego (2010), however, that C is not a proper statistics as it is based on ratios of standard deviations and not on ratios of variances; only the latter are distributed in such a way that χ^2 tests can be used to assign proper confidence levels. He shows that the standard F-statistics, where

$$F = \frac{\sigma^2(\text{blazar} - \text{star}_i)}{\sigma^2(\text{star}_i - \text{star}_j)}, \quad (1)$$

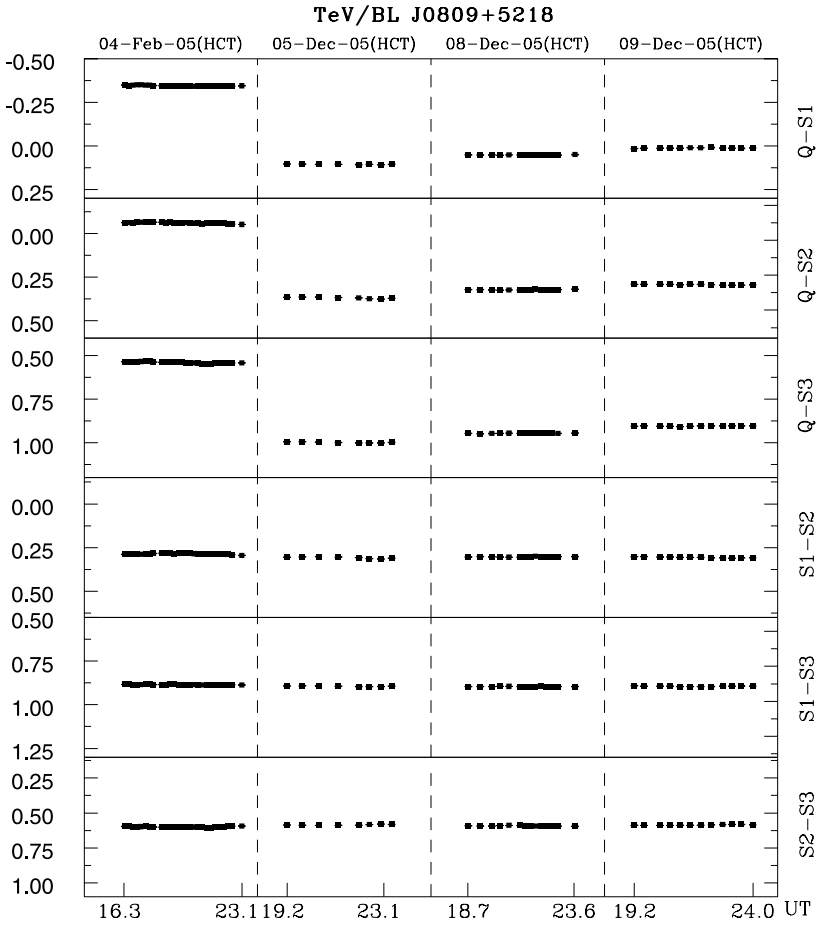

Figure 2. Long-term optical variability DLCs of the TeV blazars in set 1 (see text).

is a more appropriate choice for characterizing AGN light curves. It also has the advantage that the somewhat uncertain parameter, η, cancels out. Column 12 gives the F-value for each night along with the number of degrees of freedom shown in parentheses. Since we can compute the F-statistics only for our data, for the bulk of blazars in set 2 (not observed by us) only the C-values are available. In computing the F-values we examined the various star–star light curves to decide if any of the comparison stars might have even slightly varied on that night. We considered the steadiest two of the three comparison stars and selected the one closer to the blazar in apparent magnitude. The two DLCs (namely blazar–star and star–star) involving the selected comparison star were then used in the F-test (equation 1). For a fair comparison to the C-test, we take for the F-test a significance of >0.99 to correspond to a definitely variable source (V) and a significance between 0.95 and 0.99 to correspond to the PV classification. These indicators of variability status as computed using F-test are tabulated in the 13th column. The last column gives the reference(s) for the INOV data used here.

The peak-to-peak INOV amplitude is calculated using the definition (Romero et al. 1999)

$$\psi = \sqrt{(D_{\max} - D_{\min})^2 - 2\sigma^2}, \tag{2}$$

with $D_{\max}$ = maximum in the AGN's differential light curve, $D_{\min}$ = minimum in the AGN's differential light curve and $\sigma^2 = \eta^2\langle\sigma_{\rm err}^2\rangle$.

The INOV duty cycle (DC) for our entire sample of 22 TeV blazars (Table 3) was then computed following the definition of Romero et al. (1999; see also Stalin et al. 2004a):

$$\mathrm{DC} = 100\frac{\sum_{i=1}^{n} N_i(1/\Delta t_i)}{\sum_{i=1}^{n}(1/\Delta t_i)}\ \text{per cent}, \tag{3}$$

where $\Delta t_i = \Delta t_{i,\rm obs}(1+z)^{-1}$ is the duration of the blazar monitoring session on the ith night, corrected for the blazar's cosmological redshift, z. Note that since the monitoring durations for any given source on different nights were not equal, the computation of the DC has been weighted by the actual monitoring duration Δt_i on the ith night. The parameter N_i was set equal to 1 if INOV was detected; otherwise $N_i = 0$.

We realize that two of our nine blazars in set 1 lie at rather small redshifts (Table 1; J1221+2813 at $z = 0.102$ and J1428+4240 at $z = 0.129$), raising the possibility of a significant contribution from the host galaxy to the flux falling within the circular photometry aperture centred at the blazar. As stressed by e.g. Cellone, Romero & Combi (2000), the host's varying contribution to the flux within the aperture changes as the seeing varies and thus the atmospheric seeing changes can yield spurious INOV detection. The paper also presents simulated DLCs for the AGN, relative to a suitable comparison star, for cases where the emission from the AGN host galaxy (elliptical or spiral) is comparable to that from the AGN itself and the atmospheric seeing undergoes a large intranight variation. For a wide range in the host galaxy size, they find that even if the host's flux is comparable to that of the AGN (an extreme situation from the perspective of the present sample), the DLCs show a negligible variation ($\psi < 1$ per cent) as long as the aperture radius exceeds

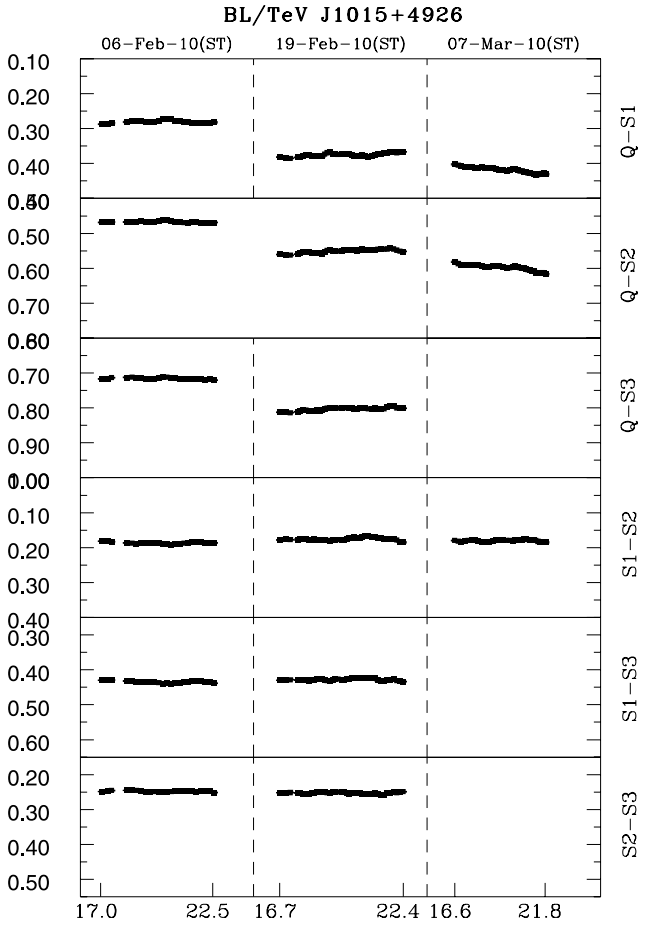

Figure 2 – *continued*

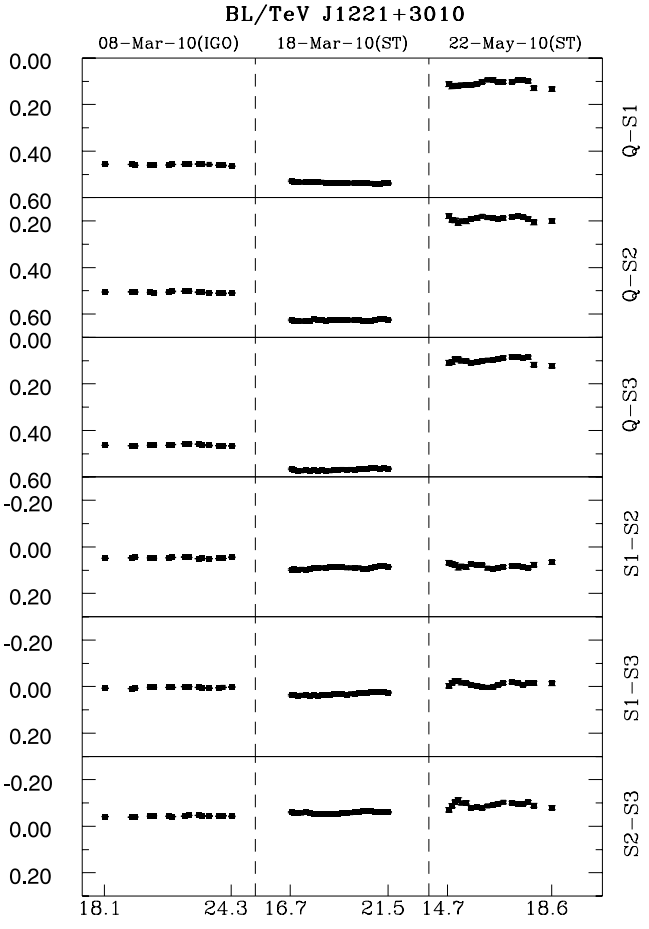

Figure 2 – *continued*

∼3–4 arcsec and the seeing remains within this limit (as also applicable to the present study). Therefore, since our choice of aperture size always meets this condition, we do not expect any of our DLCs classified as 'V' to be spurious, i.e. being an artefact of variable atmospheric seeing during the night.

Note also that in a very small number of cases the INOV results taken from the literature were for the *V* band; however, for the present purpose we do not distinguish them from our data which were essentially always taken in the *R* band.

Based on the *C*-test, the computed INOV DC for our sample of 22 TeV blazars is found to be ∼59 per cent (116 nights; Table 3), which increases to ∼64 per cent if five 'PV' cases of 'probable' INOV are also included. However, for the nights showing larger INOV amplitudes, $\psi > 0.03$, the INOV DC is ∼47 per cent. Since the redshift of the blazar J1555+1111 is known to be controversial, with values ranging from 0.25 to 0.50 (see Treves, Falomo & Uslenghi 2007 and MAGIC collaboration: Albert et al. 2008) we have computed the DC values for our entire sample of blazars (116 nights), taking the lower and upper z values for J1555+1111. The computed values are DC = 58.6 and 58.9 per cent, respectively. Thus, the uncertainty in z of J1555+1111 does not significantly affect the estimated DC for the sample (i.e. DC ∼ 59 per cent). Using the *F*-test, corresponding DC values for the sixteen blazars monitored presently is ∼72 per cent (∼76 per cent, if the two 'PV' cases are included) but only ∼33 per cent for the cases having $\psi >$ 0.03 (55 nights; Table 3).

4.2 Notes on the optical light curves of the TeV blazars

4.2.1 Set 1

The basic parameters for all the nine blazars monitored by us have been taken from the compilations by Abdo et al. (2010a) and Weekes (2008), and their INOV and LTOV light curves determined in the present work are shown in Figs 1 and 2, respectively. As seen from Table 1, the set 1 of TeV blazars consists of five high-peaked BL Lac objects (HBLs), two intermediate-peaked BL Lac objects (IBLs), one low-peaked BL Lac object (LBL) and one flat-spectrum radio quasar (FSRQ).

(i) J0222+4302 (3C 66A; $z = 0.444$). This blazar (Bramel et al. 2005) has been classified as an IBL whose non-thermal emission peaks in the range 10^{15}–10^{16} Hz (Perri et al. 2003). During 1998–2000 it was monitored in our programme on seven nights for durations ranging between 5 and 10 h per night. INOV was detected on six nights (Sagar et al. 2004). The only subhour feature seen in those DLCs is a 1.5 per cent 'glitch' detected on the night of 1999 November 13 at 19.6 UT. In Table 3, we have combined those published data with the two DLCs obtained in the present work. Of these, the DLC on 2009 September 28 showed confirmed INOV using both $C_{\rm eff}$- and *F*-statistics. Also, a clear event of *internight* variability was observed when the source faded by ∼0.04 mag between 2009 September 27 and 28 (Fig. 1).

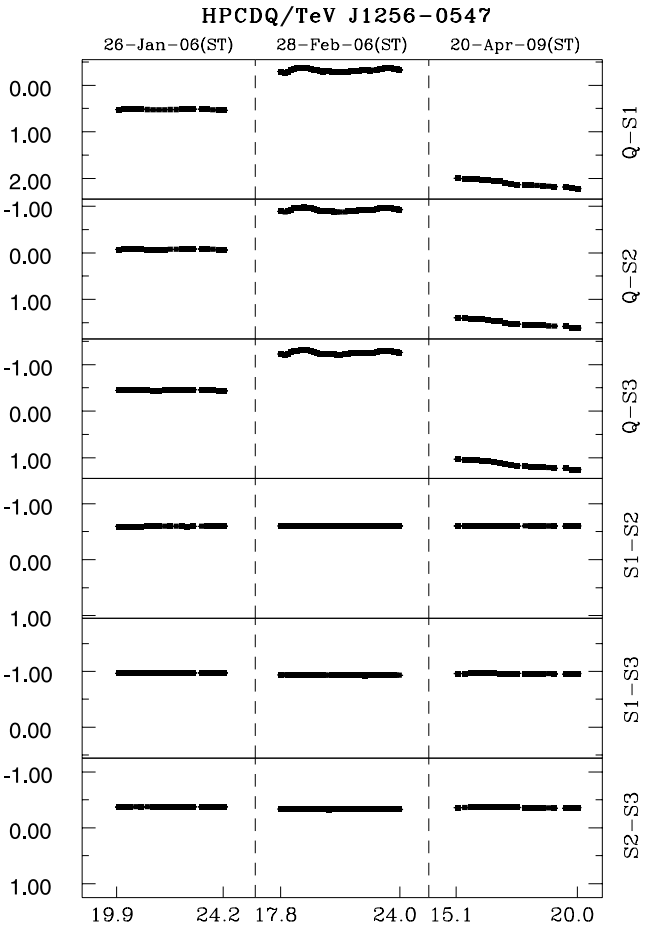

Figure 2 – *continued*

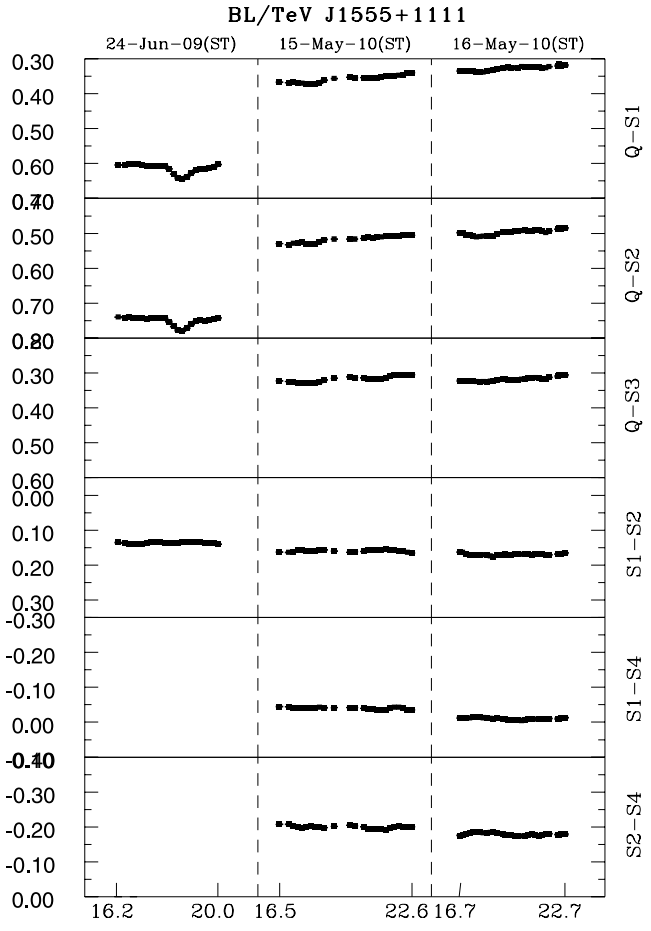

Figure 2 – *continued*

(ii) J0721+7120 (S5 0716+714; $z = 0.31$). This blazar with an 'LBL' classification is the archetypal intraday variable (e.g. Wagner et al. 1996) with a history of frequent high-amplitude flux variations (e.g. Gupta et al. 2008, and references therein). From their *R*-band light curves Wagner et al. (1996) had reported a significant 'flickering' on time-scale as short as ≈15 min. Recently, its high temporal resolution study revealed quasi-periodic oscillations of about 15 min at $>3\sigma$ significance (Rani et al. 2010). The presence of such short time-scales in an optical light curve can provide important clues to relativistic beaming at these wavelengths (e.g. Fabian & Rees 1979; Guilbert, Fabian & Rees 1983). During 1994 February and March this blazar was the target of a four-week-long INOV monitoring campaign (BVRI) under our programme, using two Indian telescopes: the 1-m ST and the 2-m Vainu Bappu Telescope (Sagar et al. 1999). Ghisellini et al. (1997) have reported a multi-colour optical monitoring campaign around that time, revealing a moderately active state of this blazar. In the Indian campaign, a monitoring duration of 2–3 h was typically achieved on each night. No evidence was found for INOV on time-scale shorter than 1 h, but 3 prominent events on ∼3 h time-scales were detected. Also, *internight* variability with $\psi \sim 5$–20 per cent was frequently detected during the 4-week-long Indian campaign. Results from other recent monitoring campaigns on this source performed at different sites should be available soon (Webb & Gupta, private communications).

The present one night's monitoring of this blazar detected a clear flare lasting ≈1 h (Fig. 1; Table 3). However, since the 1.5 h duration of our monitoring is much less than our selection criterion of $\gtrsim$4 h, we have not included this observation in the computation of DC for this blazar (Table 3). Note that neither of the aforementioned published observational campaigns revealed INOV time-scale $\tau <$ 1 h, even for this highly variable blazar, except for results reported by Wagner et al. (1996) and some recent observations reported by Rani et al. (2010).

(iii) J0809+5218 (1ES 0806+524; $z = 0.138$). To our knowledge, the present work is the first intranight optical monitoring of this HBL (four nights, Table 3). A highly unusual aspect of this source, as revealed by the 5 GHz VLBI observations, is a two-sided jet structure on parsec scale straddling the core (Chen et al. 2006), which itself has a brightness temperature of $\sim 10^{10}$ K, markedly lower than the inverse Compton limit (Kellermann & Pauliny-Toth 1969). These unusual characteristics are, however, consistent with the absence of strong relativistic boosting in this HBL, as also reflected by its quite stable GeV flux (Chen et al. 2006). On none of the four nights did we detect INOV in this blazar (Table 3), although on a longer term (∼10 month time-scale), a clear fading by ∼0.45 mag was detected. Thereafter, a distinct brightening by ∼0.04 mag occurred between the observations taken four days apart (Fig. 3).

(iv) J1015+4926 (1ES 1011+496; $z = 0.212$). Out of the three nights observed by us this HBL showed a clear variability on one night, as confirmed by both $C_{\rm eff}$- and *F*-statistics (Table 3; 2010 March 7). On the night of 2010 February 19, it was found to be a PV using $C_{\rm eff}$ but classified as 'V' on application of *F*-statistics. On a longer time-scale, a steady fading by ∼0.11 mag was seen over the one-month span covered by our monitoring (Fig. 3).

Table 3. Summary of observations and INOV results.

Source	Set no.	Epoch (dd.mm.yy)	Tel. used	Fil.	Dur. (h)	$N_{\rm points}$	σ (per cent)	ψ (per cent)	$C_{\rm eff}$	Status[a] (C-test)	F-value (d.o.f.[b])	Status[a] (F-test)	Ref.[c]
(1)	(2)	(3)	(4)	(5)	(6)	(7)	(8)	(9)	(10)	(11)	(12)	(13)	(14)
J0222+4302	1	14.11.98	ST	R	6.5	118		5.4	6.0	V			(a)
		13.11.99	ST	R	5.7	123		5.5	>6.6	V			(a)
		24.10.00	ST	R	9.1	73		4.3	5.8	V			(a)
		26.10.00	ST	R	10.1	82		3.2	3.5	V			(a)
		01.11.00	ST	R	9.0	103		2.2	2.9	V			(a)
		24.11.00	ST	R	5.1	71				N			(a)
		01.12.00	ST	R	5.1	59		8.0	>6.6	V			(a)
		27.09.09	ST	R	4.1	34	0.28	1.0	1.6	N	1.15(33)	N	(b)
		28.09.09	ST	R	6.2	38	0.19	1.1	2.6	V	3.75(37)	V	(b)
J0238+1637	2	27.10.90		V	4.5		1.00	5.0		V			(c)
		29.10.90		V	8.3		1.20	18.0		V			(c)
		05.11.91		R	6.3		1.20	20.0		V			(c)
		07.11.91		R	8.0		1.20	5.0		V			(c)
		08.11.91		R	9.4		1.30	16.0		V			(c)
		03.11.99		V	6.7		1.40	27.3	10.0	V			(d)
		04.11.99		V	6.6		1.20	24.5	6.1	V			(d)
		05.11.99		V	7.0		1.20	34.5	8.9	V			(d)
		06.11.99		V	6.7		0.70	11.0	4.4	V			(d)
		07.11.99		V	6.6		0.90	44.3	14.4	V			(d)
		12.11.99	ST	R	6.6	39		12.8	6.6	V			(a)
		14.11.99	ST	R	6.2	34		10.2	3.2	V			(a)
		22.10.00	ST	R	7.9	39		7.6	2.6	V			(a)
		22.12.00		V	7.2		0.70	7.0	3.3	V			(d)
		18.11.03	HCT	R	7.4	39	0.40	6.8	>5.54	V	58.71(38)	V	(e)
J0423−0120	2	19.11.03	ST	R	6.3	36	0.25	1.6	3.60	V	7.81(35)	V	(e)
		08.12.04	ST	R	6.0	11	0.26	1.8	0.96	N	10.51(10)	V	(e)
		25.10.09	ST	R	4.0	18	0.38	2.9	2.00	PV	6.45(17)	V	(e)
J0721+7120	1	23.03.04		R	7.0			6.0		V			(f)
		01.02.05	ST	R	1.5	24	0.25	3.1	5.1	V	22.15(23)	V	(b)
		12.01.07		R	3.6	185	0.70	6.3	2.8	V			(g)
		20.03.07		R	4.2	195	0.50		1.6	N			(g)
J0738+1742	2	26.12.98	ST	R	7.8	49		1.8	1.13	N			(a)&(h)
		30.12.99	ST	R	7.4	64		1.0	0.61	N			(a)&(h)
		25.12.00	ST	R	6.0	42		1.6	1.02	N			(a)&(h)
		25.12.01	ST	R	7.3	43		1.0	2.8	V			(a)&(h)
		20.12.03	HCT	R	5.8	36	0.23	1.0	1.78	N	1.86(35)	N	(h)
		10.12.04	ST	R	5.8	28	0.16	1.3	3.00	V	8.40(27)	V	(h)
		23.12.04	ST	R	5.0	11	0.10	1.2	3.10	V	17.83(10)	V	(h)
		02.01.05	ST	R	4.9	20	0.22	0.8	0.97	N	1.42(19)	N	(h)
		05.01.05	ST	R	5.8	23	0.15	1.0	2.25	PV	7.00(22)	V	(h)
		09.01.05	ST	R	6.7	28	0.19	1.3	3.20	V	9.78(27)	V	(h)
		09.11.05	ST	R	3.8	17	0.17	0.7	2.00	PV	3.35(16)	PV	(h)
		16.11.06	ST	R	4.5	19	0.29	1.1	0.95	N	4.35(18)	V	(h)
		29.11.06	ST	R	5.8	26	0.19	1.0	0.83	N	3.42(25)	V	(h)
		17.12.06	ST	R	5.6	24	0.19	0.9	1.06	N	5.72(23)	V	(h)
		15.12.07	ST	R	6.6	28	0.29	1.9	3.53	V	10.37(27)	V	(h)
		16.12.07	ST	R	6.6	27	0.19	1.0	1.45	N	3.87(26)	V	(h)
		22.11.08	ST	R	5.6	27	0.19	0.8	0.33	N	1.84(26)	N	(h)
J0739+0137	2	05.12.05	HCT	R	5.3	10	0.38	3.4	2.93	V	36.84(9)	V	(e)
		06.12.05	HCT	R	6.0	09	0.54	3.1	3.50	V	6.23(8)	V	(e)
		09.12.05	HCT	R	5.5	14	0.54	1.3	0.38	N	1.45(13)	N	(e)
J0809+5214	1	04.02.05	HCT	R	6.8	27	0.20	1.2	2.31	PV	1.86(26)	N	(b)
		05.12.05	HCT	R	4.3	08	0.24	0.8	0.59	N	3.40(7)	N	(b)
		08.12.05	HCT	R	4.9	14	0.11	0.4	0.15	N	1.45(13)	N	(b)
		09.12.05	HCT	R	4.8	12	0.24	0.5	0.32	N	1.27(11)	N	(b)
J0854+2006	2	29.12.98	ST	R	6.8	19		2.3	2.80	V			(a)
		31.12.99	ST	R	5.6	29		3.8	6.50	V			(a)
		28.03.00	ST	R	4.2	22		5.0	5.80	V			(a)

Table 3 – *continued*

Source	Set no.	Epoch (dd.mm.yy)	Tel. used	Fil.	Dur. (h)	$N_{\rm points}$	σ (per cent)	ψ (per cent)	$C_{\rm eff}$	Status[a] (C-test)	F-value (d.o.f.[b])	Status[a] (F-test)	Ref.[c]
(1)	(2)	(3)	(4)	(5)	(6)	(7)	(8)	(9)	(10)	(11)	(12)	(13)	(14)
		17.02.01	ST	R	6.9	48		2.8	2.70	V			(a)
		05.02.05	HCT	R	7.7	40	0.23	0.8	1.69	N	2.57(39)	V	(b)
		12.04.05	ST	R	4.1	54	0.32	7.5	5.20	V	71.39(54)	V	(b)
J1015+4926	1	06.02.10	ST	R	5.5	24	0.25	1.0	0.98	N	2.08(23)	N	(b)
		19.02.10	ST	R	5.6	41	0.30	1.8	2.17	PV	5.06(40)	V	(b)
		07.03.10	ST	R	5.2	34	0.36	3.4	4.30	V	11.99(33)	V	(b)
J1058+0133	2	25.03.07	ST	R	5.8	11	0.12	2.0	3.20	V	58.56(10)	V	(e)
		16.04.07	ST	R	3.8	15	0.17	0.8	0.53	N	1.37(14)	N	(e)
		23.04.07	ST	R	4.4	10	0.23	1.8	2.57	V	12.51(9)	V	(e)
J1159+2914	2	19.01.94		R	4.0		0.90	12.0		V			(c)
		20.01.94		R	5.5		0.80	3.0		V			(c)
		21.01.94		R	5.1		0.90	10.0		V			(c)
		22.01.94		R	5.4		1.10	11.0		V			(c)
		23.01.94		R	5.1		1.00	4.0		V			(c)
		24.01.94		R	4.0		1.30	7.0		V			(c)
J1217+3007	2	20.03.99	ST	R	7.0	21		3.50	5.50	V			(a)
		25.02.00	ST	R	5.9	28				N			(a)
		31.03.00	ST	R	5.0	27				N			(a)
		19.04.02	ST	R	6.8	23		1.80	4.90	V			(a)
J1218−0119	2	11.03.02	ST	R	8.0	22		7.3	3.20	V			(a)
		13.03.02	ST	R	8.5	24		3.8	2.60	V			(a)
		15.03.02	ST	R	3.9	11		5.5	3.50	V			(a)
		16.03.02	ST	R	8.2	22		14.1	>5.54	V			(a)
J1221+3010	1	08.03.10	IGO	R	6.2	15	0.24	0.9	1.18	N	1.96(14)	N	(b)
		18.03.10	ST	R	4.7	25	0.49	1.0	0.26	N	2.12(24)	N	(b)
		22.05.10	ST	R	3.9	19	0.88	3.3	0.41	N	2.23(18)	PV	(b)
J1221+2813	1	19.03.04	HCT	V	5.4	74	0.32	5.2	>5.54	V	16.65(72)	V	(b)
		20.03.04	HCT	V	6.6	97	0.49	8.2	>5.54	V	62.42(96)	V	(b)
		18.03.05	ST	R	4.0	26	0.33	2.0	1.74	N	3.21(25)	V	(b)
		05.04.05	ST	R	6.9	38	0.20	3.2	4.50	V	27.71(37)	V	(b)
J1256−0547	1	26.01.06	ST	R	4.2	19	0.17	2.5	>5.54	V	13.59(18)	V	(b)
		28.02.06	ST	R	6.1	40	0.25	10.2	>5.54	V	403.89(39)	V	(b)
		20.04.09	ST	R	4.9	20	0.44	22.0	>5.54	V	1069.51(19)	V	(b)
J1310+3220	2	26.04.00	ST	R	5.6	16				N			(a)
		17.03.02	ST	R	7.7	19		3.4	3.1	V			(a)
		24.04.02	ST	R	5.8	14				N			(a)
		02.05.02	ST	R	5.1	15				N			(a)
J1428+4240	1	21.04.04	HCT	V	5.8	32	0.46	2.8	1.82	N	2.90(31)	V	(b)
		22.04.09	ST	R	4.0	16	0.37	1.1	0.28	N	1.99(15)	N	(b)
		29.04.09	ST	R	6.4	27	0.73	2.1	0.65	N	1.42(26)	N	(b)
J1512−0906	2	28.04.98		V	3.8		0.30			N			(i)
		29.04.98		V	4.0		0.40			N			(i)
		30.04.98		V	4.0		0.80	4.2	1.45	N			(d)
		06.06.99		V	7.2		0.90	3.4	1.05	N			(d)
		07.06.99		V	7.3		0.90	4.2	1.27	N			(d)
		14.06.05	ST	R	4.0	09	0.12	1.6	1.53	N	12.02(8)	V	(e)
		01.05.09	ST	R	5.6	22	0.31	4.7	2.63	V	29.85(21)	V	(e)
		20.05.09	ST	R	4.8	23	0.43	3.1	0.98	N	4.20(22)	V	(e)
J1555+1111	1	05.05.99	ST	R	3.6	20		2.3	>6.60	V			(i)
		06.06.99	ST	R	7.1	40				N			(i)
		24.06.09	ST	R	3.8	23	0.17	4.2	>5.54	V	50.81(22)	V	(b)
		15.05.10	ST	R	6.1	25	0.29	2.8	>5.54	V	12.99(24)	V	(b)
		16.05.10	ST	R	6.1	31	0.30	2.3	4.63	V	6.33(30)	V	(b)
J2225−0457	2	29.09.88		R	4.8		0.80	9.0		V			(c)
		01.10.88		R	6.7		0.90			N			(c)
		08.10.10		R	5.1	16	0.64	6.8	1.12	N	14.35(15)	V	(e)
J2253+1608	2	12.09.90		R	6.9		1.00	6.0		V			(c)
		13.09.90		R	7.5		1.10	4.0		V			(c)

[a]V = variable, N = non-variable, PV = probable variable.
[b]d.o.f. = degrees of freedom.
[c]Reference for INOV data: (a) Sagar et al. (2004); (b) Present work; (c) Noble (1995); (d) Romero et al. (2002); (e) Goyal et al. (2011); (f) Pollock, Webb & Azarnia (2007); (g) Gupta et al. (2008); (h) Goyal et al. (2009); (i) Stalin et al. (2005).

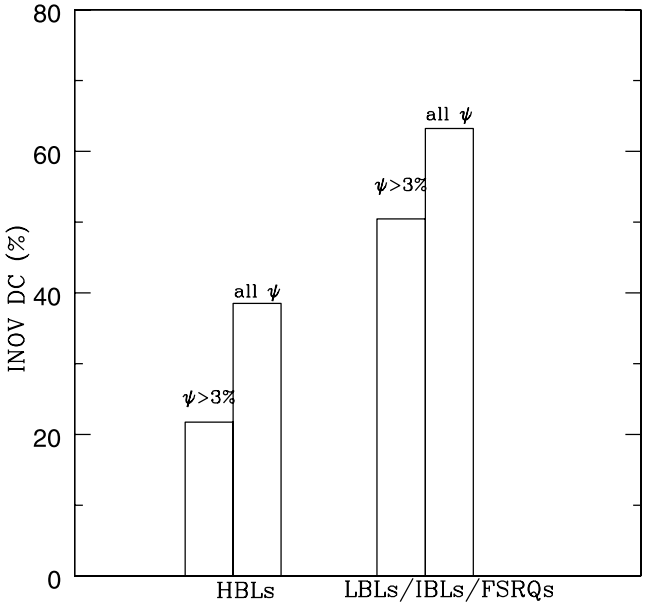

Figure 3. Histogram of the INOV duty cycle (present work) derived for the different blazar classes, for two ranges of INOV fractional amplitude ψ.

(v) J1221+3010 (1ES 1218+304; $z = 0.182$). Out of three nights observed by us this blazar showed a hint of variability on one night on applying the F-statistics, but remained non-variable on all the three nights, according to the $C_{\rm eff}$-criterion (Table 3). However, on a longer term, we detected a clear fading by ∼0.1 mag between the first two epochs, which were separated by 10 d. This was followed by a phase of 0.4 mag brightening over ∼2 months, when it was last monitored by us (Fig. 3).

(vi) J1221+2813 (W Comae/ON231, $z = 0.102$). This is the nearest source in our sample and also the first IBL to be detected at TeV energies. Gupta et al. (2008) have reported R-band monitoring of this blazar on 2007 January 11 for 3.24 h, but no INOV was detected. We monitored this blazar on four epochs. It showed a confirmed variablity on three epochs using $C_{\rm eff}$ and on all four epochs when the F-test was applied (Table 3). In addition, a clear event of *internight* variation was seen when the source faded by ∼0.1 mag between 2004 March 19 and 20.

(vii) J1256−0547 (3C 279, $z = 0.536$). This FSRQ of the optically violently variable (OVV) type was the first blazar to be detected as an EGRET/γ-ray source (Hartman et al. 1992) and the first FSRQ to be detected at very high energies (VHE, i.e. >100 GeV) (MAGIC collaboration: Albert et al. 2008). This source is also particularly interesting because with a redshift of 0.538, it is the most distant VHE blazar yet found (Abdo et al. 2009); a strong absorption of its VHE emission due to extragalactic background light is expected, yet not seen (e.g. Costamante et al. 2009). Gupta et al. (2008) have reported R-band intranight monitoring with the 1-m Yunnan observatory telescope on two nights in early 2007 (for durations of 4 and 2.3 h), but INOV was not detected. A negative result was also reported by Romero et al. (2002) from their V-band intranight monitoring lasting 3.8 h on 1999 August 6.

Application of either of the two statistics shows it to be a confirmed variable on all the three nights it was monitored by us, attaining peak-to-peak INOV amplitudes of 4, 10 and 22 per cent, respectively (Table 3). Furthermore, the blazar brightened by ∼0.9 mag between the first two epochs of monitoring that were separated by about two months, and was about 2.0 mag fainter when last observed a little more than three years later (Fig. 3).

(viii) J1428+4240 (H1426+428, $z = 0.129$). This weak TeV source has its synchrotron emission peak at the highest frequency known for any blazar; hence it is termed as 'extreme' HBL (Aharonian et al. 2002; also, Costamante et al. 2001). Its radio structure consists of a core surrounded by a faint halo (Giroletti et al. 2004). The light curves presented here are its first intranight optical monitoring observations. The $C_{\rm eff}$ values indicated that it was non-variable on all three nights we monitored it; however, on application of the F-test it was found to be variable on one of the three nights (Table 3).

(ix) J1555+1111 (PG 1553+113, $z = 0.360$). This most distant HBL with a firm TeV detection (Abdo et al. 2009) is known to show a highly time-dependent variability behaviour at different frequencies. Its radio structure is marked by an extremely large bend (by ∼110°) of the parsec-scale jet towards the outer lobe (Rector, Gabuzda & Stocke 2003). It showed INOV on one of the two nights it was monitored during mid-1999 as part of our INOV programme (Stalin et al. 2005). Those data have been included in our computation of the INOV DC (Table 3). In our monitoring, confirmed variability was detected on all the three nights both using $C_{\rm eff}$- and F-statistics. In the longer term, a clear brightening by ∼0.25 mag was observed between the first two epochs of our monitoring, which were separated by almost a year. A clear case of *internight* variability also occurred when the source brightened by another ∼0.04 mag between 2010 May 15 and 16 (Fig. 3).

4.2.2 *Set 2*

Set 2 consists of one HBL, three LBLs, eight FSRQs and one BL Lac object of unspecified HBL/LBL classification. Their INOV and LTOV data are available in the literature cited in Table 3. Only for OJ 287 do we present here new monitoring data taken by us on two nights (Table 3; Fig. 1).

(i) J0238+1637 (AO 0235+164; $z = 0.940$). This LBL had been monitored by Noble (1995) on five nights and later on three nights in the first part of our programme (Sagar et al. 2004). On all the eight nights it was found to be a confirmed variable, with ψ ranging between 5 and 20 per cent (Table 3). Romero et al. (2002) monitored it on other six nights and found ψ to range between 7 and 44 per cent. In addition, Goyal et al. (2011) have monitored this blazar on one night, and it showed a gradual decline by ∼7 per cent during the first 6 h on that night. Thus, the INOV DC of this BL Lac is essentially 100 per cent!

(ii) J0423−0120 (PKS 0420−01; $z = 0.915$). This blazar has been newly monitored by us on three nights, covering a time-span of seven years (Goyal et al. 2011). It showed a confirmed variability on 2003 November 19, with an INOV amplitude of $\psi \sim 2$ per cent and was a 'PV' on 2009 October 25 (C-test). The F-test shows it to be a confirmed variable on all the three nights. As for LTOV, it faded by ∼1.9 mag between the first two epochs of monitoring roughly a year apart and then brightened by ∼0.8 mag when we last monitored it on 2009 October 25.

(iii) J0738+1742 (PKS 0735+178; $z > 0.424$). This blazar is a rather unique case of relative intranight quiescence that has persisted over the past two decades (Goyal et al. 2009; Britzen et al. 2010), although mild INOV ($\psi < 3$ per cent) was detected on five out of the total 17 nights. On month-like time-scale it has exhibited ∼0.5 mag variations (Sagar et al. 2004; Ciprini et al. 2007; Goyal et al. 2009).

(iv) J0739+0137 (PKS 0736+01; $z = 0.191$). Not only did this highly polarized CDQ remain a confirmed variable (by both *C*- and *F*-statistics) on two of the three nights of our monitoring (Goyal et al. 2011), but it also showed a clear *internight* variability, fading by ∼4 per cent between 2005 December 5 and 6.

(v) J0854+2006 (OJ 287; $z = 0.306$). This LBL was monitored by Sagar et al. (2004) on four nights, and it showed confirmed INOV each time. It also showed large LTOV, first fading by 0.6 mag over ∼1 yr and then brightening by 1.63 mag on a two-year time-span. In Fig. 2, we present the light curves derived from our newly acquired data on two nights. The object showed a clear brightening by 7.5 per cent in 4 h on 2005 April 12. However, on 2005 February 5, it remained a non-variable (by the *C*-test), although an *F*-test showed it to be variable.

(vi) J1058+0133 (PKS 1055+01; $z = 0.888$). This FSRQ with a variable polarization was a confirmed variable on two of the three nights we monitored it (Goyal et al. 2011). It also showed a gradual brightening by ∼0.2 mag between 2007 March 25 and April 23.

(vii) J1159+2914 (4C 29.45; $z = 0.729$). Confirmed INOV was detected on all the six nights this FSRQ was monitored by Noble (1995), with ψ ranging between 4 and 12 per cent (Table 3). It has also shown large variations on *internight* time-scales. First, it brightened by 6 per cent between 1994 January 19 and 21 and then faded by ∼0.5 mag between 1994 January 21 and 22. It again brightened by 7 per cent between 1994 January 22 and 23 and was last found having faded by ∼0.3 mag on the following night.

(viii) J1217+3007 (B2 1215+30; $z = 0.130$). This blazar was monitored on four epochs by Sagar et al. (2004), showing confirmed INOV on two epochs (Table 3). Variability was also detected on a longer time-scale.

(ix) J1218−0119 (PKS 1216−01; $z = 0.554$). INOV was detected on all the four nights this blazar was monitored by Sagar et al. (2004). On longer time-scales, it showed a 2 per cent fading between the first two epochs of monitoring, followed by ∼11 per cent fading over the next two days and, finally, 14 per cent brightening within the next 24 h (Table 3).

(x) J1310+3220 (B2 1308+32; $z = 0.997$). This FSRQ showed a confirmed INOV (ψ up to 3.4 per cent) on one out of the four nights it was monitored by Sagar et al. (2004). In the longer term, it showed a strong variability (Stalin et al. 2004a).

(xi) J1510−0906 (PKS 1510-08; $z = 0.360$). This FSRQ showed confirmed INOV on two of the three nights it was monitored by us over the span of five years (Goyal et al., in preparation). In the long term, it brightened by ∼1.5 mag over the course of four years and then faded by 0.25 mag over the next 19 days when we last monitored it on 2009 May 20. In earlier INOV campaigns by Romero et al. (2002) and Stalin et al. (2005), this blazar was found to be non-variable.

(xii) J2225−0457 (3C 446; $z = 1.404$). This blazar showed INOV on one of the two nights it was monitored by Noble (1995, Table 3). On 2010 October 8 when we monitored it (Goyal et al. 2011), it was found to be non-variable using the *C*-test, but variable by the *F*-test (Table 3).

(xiii) J2253+1608 (3C 454.3; $z = 0.859$). INOV was detected on both the nights it was monitored by Noble (1995, Table 3).

5 DISCUSSION

The fairly large size of the TeV blazar sample covered in the present study and the fact that all the key blazar subclasses, namely HBL, IBL, LBL and FSRQ (Section 2; Table 1), are included in the sample, reassure us that the INOV results reported here should be representative of TeV blazars. An explicit goal of the present work, the first systematic study to define the INOV characteristics of TeV blazars, was to search for variations on subhour time-scales. As pointed out in Section 1, TeV blazars are particularly promising targets to look for such ultrarapid optical continuum variability, since their innermost jets are thought to have extremely large bulk Lorentz factors, $\Gamma \gtrsim 50$–100. Despite examining the high-quality intranight monitoring observations of all 22 TeV blazars in our sample, taken on 116 nights over a total duration of 677 h, no clear event on subhour time-scales was found, even though the data-sampling rate (typically, once every 10 min or so) was adequately dense to have revealed any such cases. This demonstrates that the occurrence of optical continuum variability on subhour like time-scales must be exceedingly rare, at least for amplitudes above ∼1 per cent, the detection threshold typically reached in the deepest INOV searches made so far. It may none the less be noted that our intranight DLCs (Fig. 1) do exhibit a few clear cases of rather sharp 'bumps', notably in the cases of J0721+7120 (2005 February 1), J1221+2813 (2004 March 20) and J1256−0547 (2006 January 26 and 28).

As mentioned in Section 1, parsec-scale radio jets in γ-ray (EGRET) blazars are known to show faster apparent (superluminal) motion as well as relatively higher brightness temperatures in their cores, compared to non-EGRET blazars (e.g. Jorstad et al. 2001; Kellermann et al. 2004; Taylor et al. 2007; Lister et al. 2009a). Indeed, in an earlier part of our INOV programme, evidence was reported for EGRET-detected blazars to exhibit a stronger INOV, again suggesting a link between INOV and the jet speed (Stalin et al. 2005). An independent evidence for such a physical link has emerged in the present study, from a comparison of the INOV DCs determined for the two major subclasses of BL Lac objects, namely 'LBLs' and 'HBLs'. The synchrotron emission from LBLs peaks in the near-infrared/optical domain, while for HBLs the synchrotron peak falls in the ultraviolet/soft X-ray regime (Urry & Padovani 1995, and references therein). Of the two classes, LBLs are known to display greater activity, and this is generally attributed to their emission being dominated by faster jets which are probably also better aligned to our direction (e.g. Ghisellini & Maraschi 1989; Sambruna, Maraschi & Urry 1996; Kharb, Gabuzda & Shastri 2008). Consistent with this picture, it has been found that LBLs display stronger INOV than do HBLs; the DC has been estimated to be ∼70 per cent for LBLs and ∼30–50 per cent for HBLs (e.g. Romero et al. 1999, 2002; see also, Heidt & Wagner 1998).

The present study allows us to check, for the first time, whether the difference persists even when the two blazar subclasses are subjected to the condition of TeV detection. From Table 1, our sample consists of seven HBLs [with the lower hump of the spectral energy distribution (SED) peaking above 10^{15} Hz] and 15 other blazars which can be together termed LBLs (see Abdo et al. 2010b; Li et al. 2010) including J1218−0119 which is a flat-spectrum core-dominated quasar. The estimated INOV DCs are 38 per cent for HBLs (26 nights' data) and 63 per cent for LBLs (90 nights' data) (Table 3). If only the cases of INOV amplitudes $\psi > 3$ per cent are considered, the DC is 22 per cent for HBLs and 50 per cent for LBLs. Both the estimates for the TeV-detected LBLs are in close agreement with those reported in Gopal-Krishna et al. (2003), for radio-selected BL Lac objects (believed to be predominantly LBLs). Fig. 3 shows the histograms of INOV DCs for HBLs and LBLs in our sample. The Kolmogorov–Smirnov test rejects at the 99 per cent confidence level the hypothesis that the two distributions are drawn from the same parent population. Thus, it is evident that the strong tendency for HBLs to show a milder INOV, vis-á-vis LBLs, persists

even if the comparison is restricted to their TeV-detected subsets. This result must be accounted for in physical models of INOV and TeV emission from blazars.

A striking outcome of our search for ultrarapid INOV is the detection of a curious, sharp feature in the light curve of the HBL J1555+1111 (on 2009 June 24; Fig. 1), the most optically luminous member of set 1 (Table 1). Intriguingly, instead of being a flare, as is more typical, this essentially symmetric feature is a clear 'dip', with an amplitude of $\sim$4.2 per cent. Its initial, falling side extends 0.5 h, and the rising side is of a slightly longer duration. We treat this detection as robust, since (i) the profile of the 'dip' is well resolved (eight data points), (ii) its peak amplitude is $>$20 times the rms noise of individual data points, (iii) the variation is visible with equal clarity and amplitude on the DLCs of the blazar against all the three comparison stars, (iv) the three comparison stars are all within 0.8 mag of the blazar, (v) all the three comparison stars remained rock steady through the monitoring duration and (vi) the atmospheric seeing too remained steady throughout the monitoring session (Fig. 1). All these points, along with the fact that in the DLCs the brightness levels seen immediately prior to and just after the dip are fairly steady and well matched, *make this feature by far the most credible, if not the only, case of an emission dip (on an hour-like time-scale) detected in the optical continuum light received from a blazar*. In addition, the blazar was substantially brighter on both other nights it was monitored by us (Table 3), making it quite unlikely that the elevated flux levels seen just before and after the dip in the light curves of 2009 June 24 are a result of multiple flares occurring at those times.

The robust detection of the dip, combined with its temporal sharpness, calls for an explanation. A plausible scenario for this rare feature would be that the optical continuum from the jet was temporarily absorbed by a foreground dusty cloud in the nuclear region. An emerging picture of AGN broad emission-line clouds suggests that they form at the distances from the central continuum source where the temperature becomes low enough for dust formation (i.e. $\sim 10^3$ K) and these dusty clouds then form a dust-driven wind (e.g. Czerny & Hryniewicz 2011; also, Krongold, Binette & Hernandez-Ibarra 2010). Recalling that the low-level detection (or non-detection) of emission lines in the case of BL Lacs could well be due to a paucity of energetic photons to ionize the gas clouds existing around the central engine (e.g. Ghisellini, Maraschi & Tavecchio 2009), it is plausible that a dusty cloud, or a stream of such clouds happens to be on our line of sight to a superluminally moving optical synchrotron 'knot' in the jet. To see if this could explain the 'dip', we need an estimate of the size of an optically emitting knot in blazar jets. Here a reasonable expectation would be that optical knots already exist in the jet before the point where the knot becomes visible in the radio band (e.g. Marscher et al. 2008), and that point typically occurs at a distance $l_{\rm rad} \approx 10^3$ times the gravitational radius of the central supermassive black hole (Lobanov 2010). For a typical supermassive black hole of mass $10^8\,{\rm M}_{\odot}$, the radio visibility point would thus be about $10^{16.5}$ cm away from the nucleus, from which a size of around 10^{15} cm can be reasonably inferred for the optical knot in the jet. The observed time-scale of the optical continuum dip ($\sim 10^3$ s), if interpreted in terms of an occultation of the superluminal knot by a dusty gaseous cloud (see above), would then require a relative transverse speed of the order of $30c$ (see Gopal-Krishna & Subramanian 1991 for such a scenario). The corresponding bulk Lorentz factor of the inner jet, $\Gamma \geq 30$ for viewing angle $\lesssim 2^{\circ}$, is not unreasonable for a TeV blazar (Section 1). One prediction of this scenario is that any such rapid intensity dips should appear more pronounced in *B*-band light curves, because of their greater sensitivity to dust obscuration, as compared to the *R*-band light curves.

Finally, searches for minute-like time-scales in the optical light curves of blazars, a key motivation for the present work, have acquired added significance in the present *Fermi*/LAT era (Atwood et al. 2009). A few recent studies of blazars have revealed a tight physical relationship between γ-ray and optical flaring events, strongly suggesting a spatial coincidence between their origins, which could well be in the jet's knot crossing a standing shock, located up to several parsecs from the central engine (see e.g. Agudo et al. 2011, and references therein). More specifically, a recent study of blazars (D'Ammando 2010) has revealed that polarized optical emission from their jets is spatially coincident with the site of the TeV flares observed on minute-like time-scales. This emerging scenario provides further motivation for more concerted efforts to search for optical variability of TeV blazars on minute-like time-scales.

ACKNOWLEDGMENTS

The authors are thankful to the anonymous referee for helpful suggestions. This research has made use of NASA/IPAC Extragalactic Database (NED), which is operated by the Jet Propulsion Laboratory, California Institute of Technology, under contract with National Aeronautics and Space Administration. We thank N. K. Chakradhari for carrying out observations for us. The authors wish to acknowledge the support received from the staff of the IAO and CREST of IIA and the IUCAA-Girawali Observatory (IGO) of IUCAA.

REFERENCES

Abdo A. A. et al., 2009, ApJ, 700, 597
Abdo A. A. et al., 2010a, ApJ, 715, 429
Abdo A. A. et al., 2010b, ApJS, 188, 405
Agudo I. et al., 2011, ApJ, 735, 10
Aharonian F. et al., 2002, A&A, 384, 23
Andruchow I., Romero G. E., Cellone S., 2005, A&A, 442, 97
Attridge J. M., Roberts D. H., Wardle J. F. C., 1999, ApJ, 518, L87
Atwood W. B. et al., 2009, ApJ, 697, 1071
Begelman M. C., Blandford R. D., Rees M. J., 1984, Rev. Modern Phys., 56, 255
Begelman M. C., Fabian A. C., Rees M. J., 2008, MNRAS, 384, L19
Bramel D. A. et al., 2005, ApJ, 629, 108
Britzen S. et al., 2008, A&A, 484, 119
Britzen S. et al., 2010, A&A, 515, 105
Carini M. T., Miller H. R., Goodrich B. D., 1990, AJ, 100, 347
Cellone S. A., Romero G. E., Combi J. A., 2000, AJ, 119, 1534
Cellone S. A., Romero G. E., Araudo A. T., 2007, MNRAS, 374, 357
Chen Y., Gu M., Shen Z.-Q., Fan Z., 2006, MNRAS, 370, 1885
Ciprini S. et al., 2007, A&A, 467, 465
Costamante L. et al., 2001, A&A, 371, 512
Costamante L., Aharonian F., Buehler R., Khangulyan D., Reimer A., Reimer O., 2009, preprint (arXiv:0907.3966)
Czerny B., Hryniewicz K., 2011, A&A, 525, 8
D'Ammando F., 2010, Invited Talk Presented at the Workshop SciNeGHE 2010, Trieste, Italy (arXiv:1012.1120)
Dai B. Z., Xie G. Z., Li K. H., Zhou S. B., Liu W. W., Jiang Z. J., 2001, AJ, 122, 2901
de Diego J. A., 2010, AJ, 139, 1269
Edelson R., Turner T. J., Pounds K., Vaughan S., Markowitz A., Marshall H., Dobbie P., Warwick R., 2002, ApJ, 568, 610
Fabian A. C., Rees M. J., 1979, MNRAS, 187
Fan J. H., Cheng K. S., Zhang L., Liu C. H., 1997, A&A, 327, 947
Ghisellini G., Maraschi L., 1989, ApJ, 340, 181

Ghisellini G. et al., 1997, A&A, 327, 61
Ghisellini G., Haardt F., Matt G., 2004, A&A, 413, 523
Ghisellini G., Maraschi L., Tavecchio F., 2009, MNRAS, 396, L105
Giannios D., Uzdensky D. A., Begelman M. C., 2009, MNRAS, 395, 29
Giroletti M., Giovannini G., Taylor G. B., Falomo R., 2004, ApJ, 613, 752
Giroletti M., Giovannini G., Taylor G. B., Falomo R., 2006, ApJ, 646, 801
Gopal-Krishna, Subramanian K., 1991, Nat, 349, 766
Gopal-Krishna, Singal A. K., Krishnamohan S., 1984, A&A, 140, L19
Gopal-Krishna, Stalin C. S., Sagar R., Wiita P. J., 2003, ApJ, 586, L25
Gopal-Krishna, Dhurde S., Wiita P. J., 2004, ApJ, 615, L81
Gopal-Krishna, Wiita P. J., Dhurde S., 2006, MNRAS, 369, 1281
Gopal-Krishna, Dhurde S., Sirkar P., Wiita P. J., 2007, MNRAS, 377, 446
Goyal A. et al., 2009, MNRAS, 399, 1622
Goyal A., Gopal-Krishna, Wiita P. J. W., Anupama G. C., Sahu D. K. S., Sagar R., 2011, submitted
Guilbert P. W., Fabian A. C., Rees M. J., 1983, MNRAS, 205, 593
Gupta A. C., Fan J. H., Bai J. M., Wagner S. J., 2008, AJ, 135, 1384
Hartman R. C. et al., 1992, ApJ, 385, L1
Heidt J., Wagner S. J., 1998, A&A, 329, 853
Helmboldt J. F. et al., 2007, ApJ, 658, 203
Impiombato D. et al., 2011, ApJS, 192, 12
Jang M., Miller H. R., 1997, AJ, 114, 565
Jannuzi B. T., Smith P. S., Elston R., 1993, ApJS, 85, 265
Jorstad S. G., Marscher A. P., Mattox J. R., Wehrle A. E., Bloom S. D., Yurchenko A. V., 2001, ApJS, 134, 181
Kataoka J. et al., 2001, ApJ, 560, 659
Kellermann K. I., Pauliny-Toth I. I. K., 1969, ApJ, 155, 71
Kellermann K. I. et al., 2004, ApJ, 609, 539
Kharb P., Gabuzda D., Shastri P., 2008, MNRAS, 384, 230
Kidger M. R., deDiego J. A., 1990, A&A, 227, L25
Kovalev Y. Y., Nizhelsky N. A., Kovalev Y. A., Berlin A. B., Zhekanis G. V., Mingaliev M. G., Bogdantsov A. V., 1999, A&AS, 139, 545
Kovalev Y. Y. et al., 2005, AJ, 130, 2473
Kovalev Y. Y. et al., 2009, ApJ, 696, L17
Krawczynski H., Coppi P. S., Aharonian F., 2002, MNRAS, 336, 721
Krongold Y., Binette L., Hernandez Ibarra F., 2010, ApJ, 724 L203
Kundt W., Gopal-Krishna, 1980, Nat, 288, 149
Kundt W., Gopal-Krishna, 2004, JA&A, 25, 115
Li H. Z., Xie G. Z., Yi T. F., Chen L. E., Dai H., 2010, ApJ, 709, 1407
Lister M. L., Homan D. C., 2005, ApJ, 130, L1389
Lister M. L., Homan D. C., Kedler M., Kellermann K. I., Kovalev Y. Y., Ros E., Savolainen T., Zensus A., 2009a, ApJ, 696, L22
Lister M. L. et al., 2009b, AJ, 138, 1874
Lobanov A. P., 2010, Mem. Soc. Astron. Ital., 81, 4
Albert J. (MAGIC Collaboration) et al., 2008, Sci, 320, 1752
Marscher A. P., 1996, in Miller H. R., Webb J. R., Noble J. C., eds, ASP Conf. Ser. Vol. 110, Blazar Continuum Variability. Astron. Soc. Pac., San Francisco, p. 248
Marscher A. P., Jorstad S. G., Mattox J. R., Wehrle A. E., 2002, ApJ, 577, 85
Marscher A. P. et al., 2008, Nat, 452, 966
Monet D. G. et al., 2003, AJ, 125, 984
Noble J. C., 1995, PhD thesis, Georgia State University
Perri M. et al., 2003, A&A, 407, 453
Petrucci P.-O., Boutelier T., Henri G., 2011, in Romero G., Sunyaev R., Bellon T., eds, Proc. IAU Symp. 275, Jets at All Scales. Cambridge Univ. Press, Cambridge, p. 122
Piner B. G., Edwards P. G., 2004, ApJ, 600, 115
Piner B. G., Pant N., Edwards P. G., 2008, ApJ, 678, 64
Pollock J. T., Webb J. R., Azarnia G., 2007, ApJ, 133, 487
Rani B., Gupta A. C., Joshi U. C., Ganesh S., Wiita P. J., 2010, ApJ, 719, L153
Rector T. A., Gabuzda D. C., Stocke J. T., 2003, AJ, 125, 1060
Romero G. E., Cellone S. A., Combi J. A., 1999, A&AS, 135, 477
Romero G. E., Cellone S. A., Combi J. A., Andruchow I., 2002, A&A, 390, 431
Sagar R., 1999, Curr. Sci, 77, 643
Sagar R., Gopal-Krishna, Wiita P. J. W., 1996, MNRAS, 281, 1267
Sagar R., Gopal-Krishna, Mohan V., Pandey A. K., Bhatt B. C., Wagner S. J., 1999, A&AS, 134, 453
Sagar R., Stalin C. S., Gopal-Krishna, Wiita P. J., 2004, MNRAS, 348, 176
Sambruna R. M., Maraschi L., Urry C. M., 1996, ApJ, 463, 444
Savolainen T., Homan D. C., Hovatta T., Kadler M., Kovalev Y. Y., Lister M. L., Ros E., Zensus J. A., 2010, A&A, 512, 24
Schlegel D. J., Finkbeiner D. P., Davis M., 1998, ApJ, 500, 525
Schlickeiser R., 1996, A&AS, 120, 481
Spergel D. N. et al., 2007, ApJS, 170, 377
Stalin C. S., Gopal-Krishna, Sagar R., Wiita P. J., 2004a, JA&A, 25, 1
Stalin C. S., Gopal-Krishna, Sagar R., Wiita P. J., 2004b, MNRAS, 350, 175
Stalin C. S., Gupta A. C., Gopal-Krishna, Wiita P. J., Sagar R., 2005, MNRAS, 356, 607
Stetson P. B., 1987, PASP, 99, 191
Stocke J. T., Morris S. L., Weymann R. J., Foltz C. B., 1992, ApJ, 396, 487
Stockman H. S., Moore R. L., Angel J. R. P., 1984, ApJ, 279, 485
Takalo L. O., Sillanpää A., Nilsson K., 1994, A&AS, 107, 497
Tanihata C., Urry C. M., Takahashi T., Kataoka J., Wagner S. J., Madejski G. M., Tashiro M., Kouda M., 2001, ApJ, 563, 569
Taylor G. B. et al., 2007, ApJ, 671, 1355
Treves A., Falomo R., Uslenghi M., 2007, A&A, 473, 17
Urry C. M., Padovani P., 1995, PASP, 107, 803
Véron-Cetty M.-P., Véron P., 2006, A&A, 455, 773
Visvanathan N., Wills B. J., 1998, AJ, 116, 2119
Wagner S. J., Witzel A., 1995, ARA&A, 33, 163
Wagner S. J. et al., 1996, AJ, 111, 2187
Webb W., Malkan M., 2000, ApJ, 540, 652
Weekes T. C., 2008, in Aharonian F. A., Hofmann W., Rieger F., eds, AIP Conf. Ser. Vol. 1085, High Energy Gamma-Ray Astronomy. Am. Inst. Phys., New York, p. 3
Wehrle A. E., Morabito D. D., Preston R. A., 1984, ApJ, 89, 336
Wiita P. J., 2006, in Miller H. R., Marshall K., Webb J. R., Aller M. F., eds, ASP Conf. Ser. Vol. 350, Blazar Variability Workshop II: Entering the GLAST Era. Astron. Soc. Pac., San Francisco, p. 183
Wills B. J., Wills D., Breger M., Antonucci R. R. J., Barvianis R., 1992, ApJ, 398, 454
Xie G. Z., Li K. H., Bai J. M., Dai B. Z., Liu W. W., Zhang X., Xing S. Y., 2001, ApJ, 548, 200

This paper has been typeset from a TEX/LATEX file prepared by the author.